Inaugural – Dissertation

zur Erlangung der Doktorwürde

der

Naturwissenschaftlich – Mathematischen

Gesamtfakultät

der

Ruprecht – Karls – Universität

Heidelberg

vorgelegt von

Diplom – Chemiker

Eric Dyrcz

aus Mannheim

Tag der mündlichen Prüfung

29.01.2016

Peptide microarrays

as

diagnostic tool

for

cancer associated protease profiling

Gutachter:

Prof. (apl.) Dr. Reiner Dahint

Priv. Doz. Dr. Ralf Bischoff

Abstract

In the human organism more than 500 proteases have been described so far. Many of them are essential in the regulation of physiological processes, as inflammation, immune response, coagulation or growth. A dysregulation in protease activity corresponds to severe malfunctions and causes numerous pathophysiological diseases, as neurodegenerative disorders, cardiovascular diseases and cancer. When it comes to cancer, proteases play an important role in progression and metastasis. Some are secreted from the tumor and can be found in the extracellular matrix of the tumor microenvironment and also in the bloodstream. Functional protease profiling aims at discovering tumor associated protease activity in clinical specimens (serum, plasma and tissue), which could be used for diagnostic and prognostic purposes. Therefore, it is necessary to find substrates, which are specifically cleaved by cancer-associated proteases. Various approaches using antibody based antigen detection or MS-based techniques, are limited in the number of samples, which can be screened in parallel. To overcome these problems, peptide microarrays were used. Compared to *Ronald Frank´s* SPOT-synthesis, micro-particle solid phase peptide synthesis (mpSPPS) allows much higher peptide densities with up to 1000 different peptides per cm^2, dependent on the layout. This PhD thesis dealt with the development of a high-throughput screening assay platform based on in-situ synthesized peptide microarrays. As first step a model system, using known proteases (trypsin, thrombin, proteinase k etc.), was developed. To check for general applicability of the PEGMA/MMA surface, on which the peptide synthesis takes place, the manufactured peptide microarrays, containing N-terminal antibody recognition sequences (FLAG- & HA-tags), were used without further chemical modification. After proteases incubation, the respective fluorescently labeled anti-FLAG- & anti-HA antibodies will only bind to peptides, bearing the intact tag-sequence, leading to a decrease in fluorescence intensity, where the enzymes were active. After demonstrating on-chip proteolysis, using indirect antibody labeling, the biotin-streptavidin system was introduced to minimize the peptide label to a smaller tag. This allowed greater sequence variability and avoided false positive cleavage, as when using a proteinogenic tag sequence. Together with the *PEPperPRINT* Company, a biotin toner was developed, to integrate this labeling reagent into the in-situ synthesis process, which turned out to be advantageous compared to in-solution modification of the peptide content. To further overcome limitations on the part of the solid support, the polymer film was optimized, by introducing a new dextran surface. Preliminary experiments in lab-scale showed good proteolytic cleavages with model proteases and spotted peptides. The transfer to production scale however, showed the

requirement of optimization, regarding polymer composition and peptide density, which is an ongoing process.

Kurzfassung

Bisher sind im menschlichen Organismus mehr als 500 Proteasen identifiziert worden. Viele von ihnen sind maßgeblich an der Regulation vieler physiologischer Prozesse, wie Inflammation, Immunabwehr, Gerinnung oder Wachstum beteiligt. Bei einer Fehlfunktion bzw. Dysregulation der Proteaseaktivität, kommt es in Folge zu gravierenden Störungen, die zu Entzündung, neurodegenerativen oder kardiovaskulären Krankheiten, bis hin zu Krebs führen können. Gerade bei Krebserkrankungen spielen Proteasen eine zentrale Rolle. Es ist bekannt, dass schon in frühen Stadien, tumor-assoziierte Proteasen sezerniert werden, die die Progression und Metastasierung des Primärtumors unterstützen und daher nicht nur im umliegenden Gewebe, sondern auch in der Blutbahn zu finden sind. Das funktionelle „Monitoring“ von Krebs-assoziierten Proteasen ist ein vielversprechender Ansatz die Proteaseaktivität in klinischem Probenmaterial (Serum, Plasma und Gewebe) zu untersuchen, um damit die Labordiagnostik von Tumorerkrankungen entscheidend zu verbessern. Die Analyse der tumor-assoziierten Proteaseaktivität ist durch die Inkubation mit geeigneten Substraten (Reporter Peptide) und dem Nachweis von spezifischen Spaltprodukten möglich. Derzeit sind Nachweissysteme auf Antigen-Antikörper Basis und massenspektrometrische Methoden weit verbreitet. Diese sind aber, aufgrund ihrer limitierten Zahl an parallel zu untersuchenden Proben, ungünstig. Um diesem Problem zu begegnen, wurden in der vorliegenden Dissertation s.g. Peptid-Mikroarrays genutzt. Im Gegensatz zu *Ronald Frank´s* SPOT-Technologie, können mittels der partikel-basierten Festphasenpeptidsynthese (mpSPPS) deutlich höhere Peptiddichten von bis zu 1000 Peptiden per cm^2, je nach Layout, realisiert werden. Es sollte im Folgenden eine Mikroarray-basierte Screening-Plattform etabliert werden, um Analysen im Hochdurchsatzformat durchführen zu können. Im ersten Schritt wurde ein Modellsystem unter Benutzung bekannter Proteasen entwickelt (Trypsin, Thrombin, Proteinase K etc.). Um die generelle Funktionsfähigkeit der benutzten PEGMA/MMA funktionalisierten Mikroarrays für diese Anwendung zu überprüfen, wurden Träger mit N-terminalen antikörperspezifischen Tag-Sequenzen (FLAG- & HA-tag) produziert. Ohne weitere chemische Modifikation, wurde eine Proteaseinkubation vorgenommen und anschließend zur Detektion eine Immunfärbung mit fluoreszenzmarkierten anti-FLAG und anti-HA Antikörpern durchgeführt. Diese binden nur vollständig intakte Tag-Sequenzen und zeigen daher eine Abnahme der Fluoreszenzintensität in den Peptidspots, die zuvor proteolytisch gespalten wurden. Nach erfolgreicher Demonstration der enzymatischen Aktivität, wurde das Biotin-Streptavidin System eingeführt, um die Tag-Sequenz zu verkleinern. Dies sollte zum einen die kombinatorische Vielfalt der Peptidsequenz vergrößern und zum anderen falsch-positive Spaltungen durch den Ersatz der proteinogenen Erkennungssequenz verhindern. In

Zusammenarbeit mit der *PEPperPRINT GmbH*, wurde ein Biotin-Toner entwickelt, der eine In-situ-Synthese des Markierungsbausteins ermöglicht, was eine deutliche Verbesserung der Peptidmarkierung, im Vergleich zu Kopplungen aus Lösung, zeigte. Des Weiteren wurden Optimierungen der Array-Oberfläche, durch die Einführung eines Dextranfilms, angestrebt. Erste Laborexperimente zeigten gute Ergebnisse der Proteolyse mit gespotteten Peptiden und Modell-Enzymen. Der Transfer in den Produktionszyklus zeigte schließlich Optimierungsbedarf was die Polymersynthese und auch die Peptiddichte angeht; zukünftige Arbeiten werden sich mit diesen Themen beschäftigen.

Table of contents

This work was conducted from 01/2013 to 12/2015 at the *German Cancer Research Centre* (DKFZ) in Heidelberg, Germany.

I. Introduction

I.1. Peptides, Proteins & Enzymes

In all living systems biomolecules are the major players. We mainly distinguish between four groups; lipids, polysaccharides, nucleic acids and proteins. Proteins consist of small building blocks, the amino acids, which are connected via amide bonds (peptide bond), to form peptides. There are 20 naturally occurring amino acids, out of which all resulting biomolecules are built. If the resulting polypeptide chain is longer than 50 residues, we usually speak of a protein. The exact amino acid sequence is called *primary structure*. Due to internal hydrogen bond formation, proteins show a special arrangement of their amino acid residues, which is referred to as *secondary structure*. Besides the α-helix and β-sheet conformation, the two regular forms of the *secondary structure*, there are a lot more like hair-pin and coiled-coil structures. If we look at the arrangement of the entire polypeptide chain, we speak of the *tertiary structure* or *protein folding*, which is highly dependent on the surrounding conditions, for example in a cell. There, the polar residues will be exposed to the aqueous cytosol, whereas the nonpolar residues will tend to stick together in a hydrophobic-like core. The term quaternary structure characterizes the conformation of several protein subunits, which can be stabilized by hydrogen bonds or disulfide bridges between the single subunits. Hemoglobin, the iron-binding protein complex of our red blood cells, is an example for a protein with four identical subunits and an additional prosthetic group to bind oxygen. Proteins in turn can be subdivided into five groups, the structural proteins as collagen and keratin are essential for the construction of our body. Storage proteins as the already mentioned hemoglobin and ferritin are responsible for housing critical elements, our cells need. Hormonal proteins act as chemical messengers; insulin, as common example, regulates the sugar level in the blood system. Another very important class of proteins is represented by the immunoglobulins, which act as antibodies, recognize pathogens and therefore support the immune system. Finally the perhaps most important group of proteins are the enzymes. They catalyze a great number of biochemical reactions occurring in a living organism. There are six classes of enzymes shown in table 1 on the next page.

Class	Catalyzed chemical reaction	Example
Oxidoreductase	Oxidation-Reduction in which oxygen and hydrogen are gained or lost	Cytochrome oxidase, lactate dehydrogenase
Transferase	Transfer of functional groups, such as an amino, acetyl or phosphate group	Acetate kinase, alanine deaminase
Hydrolase	Hydrolysis (addition of water)	Lipase, sucrase
Lyase	Removal of groups of atoms without hydrolysis	Oxalate decarboxylase, isocitrate lyase
Isomerase	Rearrangement of atoms within a molecule	Glucose-phosphate isomerase, alanine racemase
Ligase	Joining of two molecules	Acetyl-CoA synthetase

Table 1: Classes of enzymes.

Although enzymes usually consist of hundreds of amino acids, only a few of them play a role in the actual catalytic process. This part of the protein is known as the *active site*. The overall structure of an enzyme determines the appearance of its active site. This fact allows the enzyme to address specifically its right substrate like a key fitting its lock. With their unique properties, enzymes play an important role in every living cell, from metabolic processes to signal transduction or DNA modification and many more. The systematic study of proteins concerning their structure and function in living organisms gained a great interest in the last 20 years; since 1997 we call this field *proteomics* according to genomics, the study of the genome[1]. The entire set of proteins is therefore called *proteome*[2].

I.2. Proteases & Diseases, especially cancer

Proteases, belonging to the group of hydrolases, catalyze the hydrolysis of amide bonds. Other than many reversible posttranslational modifications of proteins, like e.g. phosphorylation, proteolysis remains irreversible. Therefore proteolytic enzymes mediate processes that are themselves irreversible: coagulation, digestion, maturation of cytokines and prohormones, apoptosis and the breakdown of intracellular proteins. So proteolysis is a ubiquitous mechanism that regulates the function and fate of a protein[3]. The general mechanism, proteases are performing, is basically a nucleophilic attack on the carbonyl-carbon of an amide bond. There are five classes of proteases, depending on the active site residue or ion that carries out catalysis, namely serine, threonine, cysteine, aspartic and

metallo proteases. As figure 1 illustrates, aspartic and metallo proteases immobilize and polarize a water molecule, so that the oxygen atom of water becomes the nucleophile. Serine and cysteine proteases use their –OH and –SH side chains directly as nucleophile.

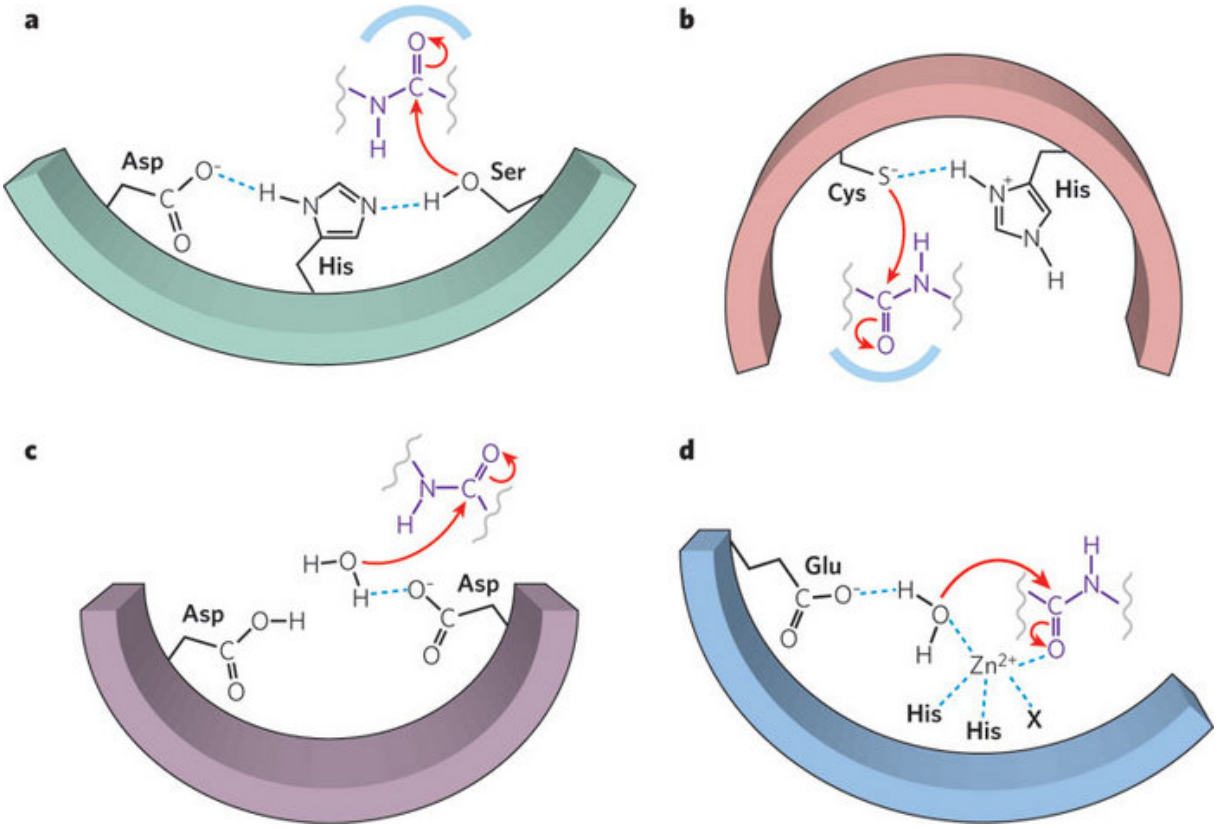

Figure 1: Schematic representation of the processes catalyzed by different classes of proteases: (a) serine protease; (b) cysteine protease; (c) aspartic protease; (d) metallo protease[1]

The degradome database lists about 569 human proteases and homologs, whereas the serine and metallo proteases are the most densely populated classes[4]. The roles of proteases range from digestive functions, the removal of damaged proteins and protein maturation to the precise processing of regulatory proteins. The architectural design of proteases ranges from small catalytic units (~20 kDa) to protein degradation machines, like the proteasome. The structural organization of a protease induces its substrate specificity, right localization in the cell, kinetic properties and sensitivity to endogenous inhibitors[5]. Providing an important link between genetics and biochemistry, proteases act as key players, for example in signaling cascades like blood coagulation, inflammation, immunity, apoptosis, and many more[6,7]. Therefore it is obvious, that alterations in proteolytic systems underlie

[1] Erez, E., Fass, D., & Bibi, E. How intramembrane proteases bury hydrolytic reactions in the membrane. *Nature* **459,** 371–378 (2009).

multiple pathological conditions such as cancer, neurodegenerative disorders, inflammatory and cardiovascular diseases[5]. So there has been an increasing interest in identification and structural characterization of proteases as potent pharmacological targets and also as diagnostic markers in the last decades[8]. Modern cancer research does not only focus on mutations in cancer cells but gained increasing interest in the extracellular matrix (ECM) of the tumor microenvironment, which has also a high impact in tumor progression[9]. MMP´s have been found to play a key role in regulating the ECM, as they can be found upregulated in almost every human cancer compared to normal tissue[10]. The relevance of proteases in the late stages of cancer has been known since a long time. Via degradation of the extracellular matrix, metastasis and tumor growth is supported dramatically. But also in early stages of a malignant tumor, proteases play an important role, for instance in modulating growth factors for the tumor progression[11]. Already today there are single cancer associated proteases with high diagnostic importance, like for example Kallikrein-related Peptidase 3, better known as prostate specific antigen (PSA), a serine protease[12,13]. Other proteases, like Urokinase Plasminogen Activator system (uPA/uPAR/PAI1), have shown to be of prognostic importance for the mamma carcinoma. uPA for example shows a correlation between the serum protease pattern and the respective primary tumor[14,15]. Also in colon cancer prognostic relevant protease profiles in primary cancer tissue could be identified relating to MMP´s and high activity/concentration of cathepsins in serum respectively[16,17]. Obviously secreted proteases from the tumor are not only present in its surrounding area but can be found also in the bloodstream[18]. Furthermore, cancer associated proteases are not only secreted by the primary tumor tissue but also from the surrounding connective tissue and also infiltrated leukocytes[19,20]. Today individual highly expressed proteases for numerous tumor entities in tissue, serum and plasma samples have been described, which are relevant for prognosis[21].

I.3. Protease profiling

The methods for identifying proteases in clinical specimen of cancer patients are nowadays based on antigen detection. However there is frequently no differentiation between zymogenes and active proteases possible[22]. This differentiation is mandatory because in most cases proteases are regulated via activation of zymogenes rather than in the gene expression level[23]. Although activity measurements are advantageous over antigen detection, only single substrates have been identified so far[24,25]. The detection of MMP-2 activity in serum samples for example can be monitored down to a concentration of 1ng/ml, by using the specific reporter peptide with the sequence *IPVSLRSG*[26]*.* When measuring

different protease activities in serum specimen in parallel in a multiplex-analysis, the sensitivity and specificity of protease profiling can be increased[26]. The major challenge is to find suitable reporter peptides, which are specifically cleaved by cancer associated protease. If the protease is available in high purified or recombinant form, specific substrates can be screened by using an in-solution or surface-based library of fluorescent labeled peptides[27,28,29]. Another problem is the limitation of the complexity of conventional peptide libraries from several hundreds to thousand substrates, due to the high costs of synthesizing fluorescently labeled peptides. This makes the identification of a sufficient number of reporter peptides difficult. However, due to the heterogeneity of the protease profiles during tumor progression and in different tumor entities, a sensitive and specific multiplex-analysis is obligatory to detect different protease activities simultaneously[25]. The utilizability of such a multiplex-analysis has been already demonstrated in model systems using caspases and cell lysates[30]. The transfer of functional protease profiling for clinical specimen like serum, tissue and plasma remains to be investigated.

I.4. Peptide arrays

In the last two decades, new technologies based on microarrays found their way into the labs, improving many biological and clinical diagnostic approaches. Today the demand of investigating complex systems in a high-throughput format increases. In genomic research, for instance, this lead to the development of DNA-microarrays, which are routinely used to screen thousands of molecules and their specific interactions with a sample in parallel. Typically those microarrays are synthesized by either lithographic, electrolytic or electrophoretic techniques[31,32,33]. Photolithographic methods are capable of producing highly ordered arrays with more than 250,000 oligonucleotides per cm^2[34]. Using randomly orders bead arrays, even higher densities over one million features per cm^2 are possible and are used for whole-genome genotyping[35,36,35,37]. However, most important interactions in vertebrates are ongoing on the proteome level, which results in a much higher complexity compared to the genome. The development of high-throughput arrays on a protein level is therefore much more challenging, due to 20 building blocks, the proteinogenic amino acids, of which all proteins are consisting of, compared to the four nucleotides in our DNA. In 2000 *MacBeath et al.* demonstrated the first protein array on a support[37,38].

The synthesis of peptide arrays, in contrast, is an easier task. Although the detection of interactions, which need extended protein regions or complex folding, is not possible, peptide arrays provide plenty of possible applications in proteomics. For example, many protein

interactions are mediated by *peptide recognition modules*, as SH2, SH3 etc. Those are peptide sequences, which are embedded in protein binding pockets[39]. Other approaches can be binding studies for antibody characterization (epitope mapping), biomarker screening or enzyme profiling.

This PhD thesis dealt with the development of an high-throughput assay system to measure enzyme activity in various samples, in order to identify new reporter peptides, specifically cleaved by cancer associated proteases.

I.5. High-density peptide arrays

In order to assemble as many peptides on a microarray as possible, early approaches focused on pre-synthesizing peptide libraries and spot them on a solid support, preferably on glass slides. Figure 2 shows the schematic workflow of the combinatorial synthesis/ SPOT-synthesis.

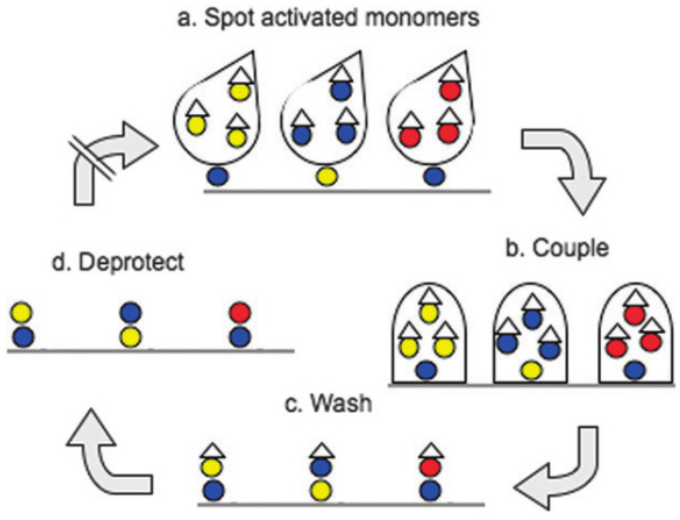

Figure 2: Schematic overview SPOT-synthesis. (a) A spotter positions the four activated bases for oligonucleotide synthesis or the 20 different C-terminally activated amino acid derivatives for peptide synthesis, all contained within liquid droplets, to defined areas on a solid support. (b) They are then coupled to this support in parallel. A cycle of synthesis is completed when (c) excess monomers are washed away and (d) the transient protection group is removed. Repetitive coupling cycles generate an array of oligonucleotides or peptides, the sequences and positions of which are known.[2]

However, the disadvantages of this method are the high cost and the technical limitations by using the SPOT-technique, resulting in maximal peptide densities of around 25 spots per cm^2[40]. Obviously small droplet volumes are difficult to handle, regarding evaporization or

[2] Breitling, F., Nesterov, A., Stadler, V., Felgenhauer, T. & Bischoff, F. R. High-density peptide arrays. Mol. Biosyst. 5, 224–234 (2009).

their spreading over the array. Ronald Frank invented peptide arrays, where the peptides are directly synthesized spot on spot on a cellulose support. This made the synthesis cheaper and even large numbers of small proteins available[41,42]. To overcome those limitations a variation of the SPOT-synthesis, the so called SC^2 method was developed[43]. Here, individual peptides are synthesized on a large cellulose area, afterwards deprotected by using TFA, which breaks down the cellulose support and small peptide-cellulose conjugates are formed. These collected conjugates can be spotted in high-density in a second step onto another solid support, like for example glass slides. This procedure allows for highly reproducible production of multiple densely spaced peptide array replicas[40]. Although patented already in 1994, high-density peptide arrays, manufactured by using an ink-jet printer, as it is done e.g. through Agilent´s SurePrint Technology for oligonucleotide arrays, have not yet been reported[44,45]. The solvents needed in peptide chemistry are thought to be problematic when it comes to ink-jet printing, due to their viscosity, which might be incompatible with this technique.

Transferring lithographic methods, originally invented to produce computer chips, to the microarray field, allowed for the first time the production of truly high-density arrays, revolutionizing first the world of genomics[31,46]. Figure 3 shows the schematic overview of this technique.

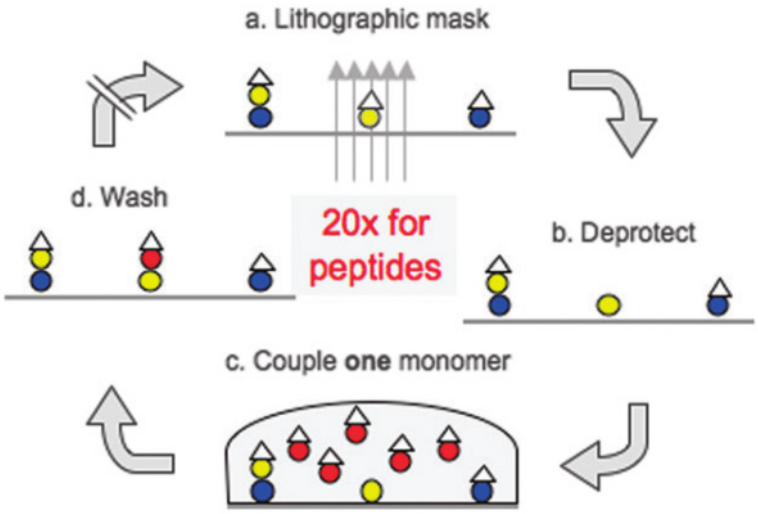

Figure 3: Lithographic synthesis. (a) A pattern of light defines first areas on a 2D solid support. (b) There, through irradiation, the transient protection group at the tip of the growing oligomer chain is removed. (c) Next, the whole support is uniformly covered with one of the 20 different C-terminally activated amino acid derivatives. These are coupled only to those structures deprotected by the previous lithographic step. (d) Excess monomers are washed away. These steps are repeated four times with the four different nucleotides or 20 times with the 20 different amino acids to add one layer during the synthesis of oligonucleotides or peptides, respectively. Repetitive coupling cycles generate an array of oligomers.[3]

[3] Breitling, F., Nesterov, A., Stadler, V., Felgenhauer, T. & Bischoff, F. R. High-density peptide arrays. Mol. Biosyst. 5, 224–234 (2009).

Fodor et al. showed, for the first time, that also peptide arrays can be manufactured by using lithographic methods[31]. One drawback is the necessity of a large number of coupling cycles. To generate a 10 mere peptide array, for instance, 20x10 cycles are needed, compared to 4x10 for a 10 mere oligonucleotide array. The difficulty is that the more coupling cycles that are performed, the more side-reactions can occur. Another disadvantage was the need of photolabile protections groups, resulting in poor coupling yields. For further information about other lithographic approaches and improvements, reference is made to the literature[32,33,47,48]. The former group *Chip-based Peptide Libraries* at the DKFZ developed a method for combinatorial synthesis of peptide arrays by using solid amino acid particles. These triboelectrical charged particles can then be positioned on a 2D-support using electrical fields by either a laser printer or on a computer chip. Up to 40,000 peptides per cm^2 are possible with this approach[29,49]. Figure 4 illustrates the schematic workflow of this particle-based synthesis with a laser printer.

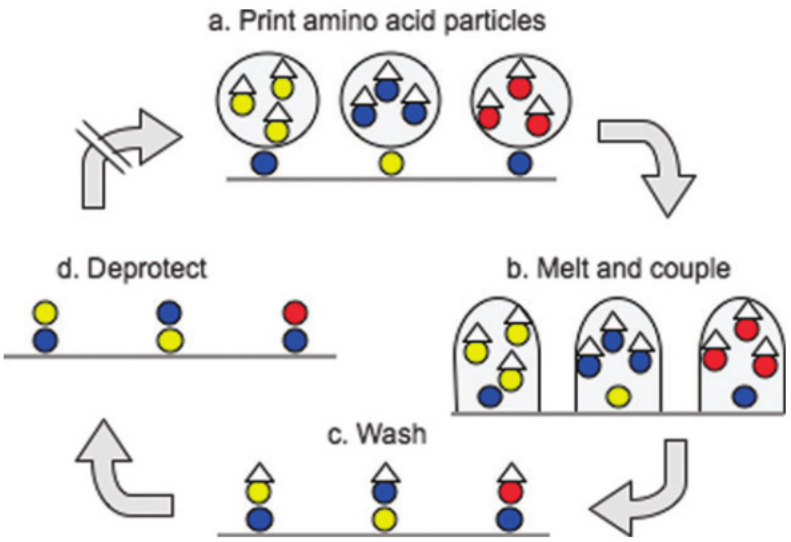

Figure 4: Positioning amino acid particles with a laser printer. (a) A laser printer positions Fmoc-amino acid-OPfp esters embedded within solid toner particles onto a solid support derivatised with free amino groups. (b) The particles are melted after transfer. As a result, oily reaction spheres are formed by surface tension. This procedure frees previously immobilized chemically activated amino acid derivatives and allows them to diffuse. At the same time, very small reaction spheres are separated from one other, allowing for elongation of growing peptides in parallel and at high density. A cycle of synthesis is complete when (c) excess monomers are washed away and (d) the Fmoc protection group is removed. Repetitive coupling cycles generate a peptide array with one coupling cycle per layer. Peptide length is determined by the number of coupling cycles.[4]

This method uses standard Fmoc-chemistry together with a solid solvent (at RT), which allows the embedding of activated (C-terminal Opfp-ester activation) amino acids within these particles[50]. The big advantages are the great stability of the activated amino acid compounds within the matrix of the particles and the possibility to consecutively position different particles next to each other onto the solid support before melting and induction of

[4] Breitling, F., Nesterov, A., Stadler, V., Felgenhauer, T. & Bischoff, F. R. High-density peptide arrays. Mol. Biosyst. 5, 224–234 (2009).

coupling[49]. The melting step gives highly viscous reaction spheres, which allow the reaction to take place restricted to its desired spot, avoiding cross-contamination. Finally this method, commercialized in the *PEPperPRINT* Company (Heidelberg, Germany), allows building up peptide arrays with up to 280,000 individual peptides. For further information about the theoretical background and the commercialized products, reference is made to the literature and the webpage of the *PEPperPRINT* Company[51].

II. Project Aims

II.1. General Idea

For solid tumors, numerous pathophysiological relevant proteases are described, which promote the progression of melanoma, including several metallo-, serine- and cysteine proteases, as well as cathepsines. For some tumor entities, proteases as diagnostic/prognostic markers have already been identified. Normally the detection of cancer associated proteases from clinical serum-, tissue- or plasma samples uses immunological approaches. Due to the absence of specific and sensitive substrates, activity measurements are not widespread. Therefore, cancer specific marker peptides have to be identified by using high-density peptide microarrays, manufactured by the *PEPperPRINT* Company, in order to screen large peptide libraries in parallel. Functional protease profiling should be performed with clinical samples from different tumors, as colon-, mamma-, pancreatic-, prostate- and lung cancer. Selected substrates, which are differential processed compared to a healthy control cohort, will be then further optimized. Finally a peptide microarray, containing all potential substrates, will be constructed for validation with various biobanks.

II.2. State-of-the-art

Since many years *Findeisen et al.* (Institute for clinical chemistry, UMM, Mannheim) deal with the analysis of clinical serum and plasma samples by using mass spectrometry (Proteomic Profiling)[52]. Especially low molecular weight peptides are generated due to proteolytic cleavage out of serum proteins[8,53]. Because of the high proteolytic activity in serum specimen, there is also a high pre-analytical variability, which makes standardization difficult. Therefore, MS-based profiling is highly limited for diagnostic applications. Even when using standardized conditions, the analysis will not lead to the identification of cancer-associated proteases, rather than cleavage products and fragments of high-abundant serum proteins[54,55,56]. The abundance discrepancies of serum proteins are in the range of 10 logarithmic levels but the dynamic measurement range of mass spectrometry is only 2-3 levels. To display low-abundant proteins, excessive fractionizing is mandatory, which cannot be done in high-throughput format; also the reproducibility is not ensured[57,58]. To overcome these problems, an excess of exogenous reporter peptides was used, in order to replace the

endogenous serum proteins, so that the reporter peptides will be preferably cleaved by cancer-associated proteases. The resulting profiles of the different processed reporter peptides represent the tumor-associated protease activity in the individual serum samples and are the basis for further clinical classification[59,60]. Protease profiling using reporter peptides can be standardized and is very sensitive, due to accumulation of cleavage products and therefore also of the signal[61]. Figure 5 shows the exemplary construction of a reporter peptide for the cancer-associated protease *Cancer Procoagulant (CP)* (EC 3.4.22.26), which is secreted by several solid tumor entities and can be found in high activity in serum samples of cancer patients[62].

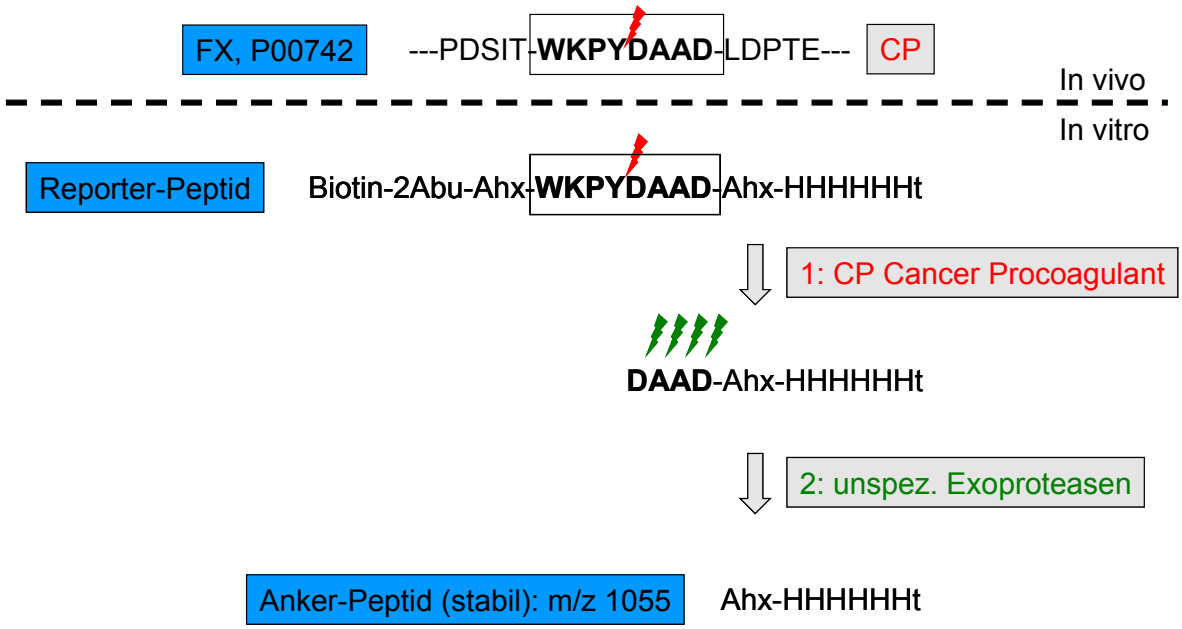

Figure 5: Example for the construction of a reporter peptide for MS-based protease profiling. From database research a peptide sequence is identified and several structural elements (affinity-tags, linker, and stop-elements) are added, which are relevant for sensitive detection via MS. After addition of the reporter peptide to the serum sample, the cleavage of the reporter peptide by the endoproteinase CP at its specific cleavage site (red lightning) begins. The resulting fragment is then cleaved by exoproteases (green lightnings) to the non-cleavable ancor-peptide with the mass 1055 [M+H$^+$]. 2Abu: 2-amino-butyric acid; Ahx: amino-hexanoic acid; t: d-threonine.[5]

So far the number of relevant substrates, which could be identified via MS, is limited, due to their low specificity in serum samples. Also the substrate specificity is a major problem in the present used assays[63]. Furthermore the number of peptides, which can be screened in parallel, is highly limited, due to the complexity of the MS data, with the increasing number of fragments.

[5] Findeisen, P.; Yepes, D. (2013)

II.3. Work Plan

In order to find new substrates, which are specific for cancer-associated protease activity, a high-throughput assay system, based on high-density peptide microarrays, has to be developed. For this purpose random peptide libraries, as well as sequences identified via database research, together with positive and negative controls will be used, to design a screening chip. The microarray manufacturing and peptide synthesis was conducted to the *PEPperPRINT* Company. Their innovative technology using a laser-printing approach to produce high-density peptide microarrays is advantageous regarding complexity and cost effectiveness. To detect and monitor proteolytic activity in a sample of interest, the peptides have to be modified with a label, which can be read out during and after enzyme incubation. The most convenient way is a fluorescent labeling of the peptides, which can be easily read-out with an appropriate scanner. Figure 6 shows the attachment of a fluorescent dye to the free N-terminus of the peptides. After proteolytic cleavage, the fragment, which bears the labeling reagent will be washed away, which leads to a reduction or even deletion in fluorescence intensity for this individual spot.

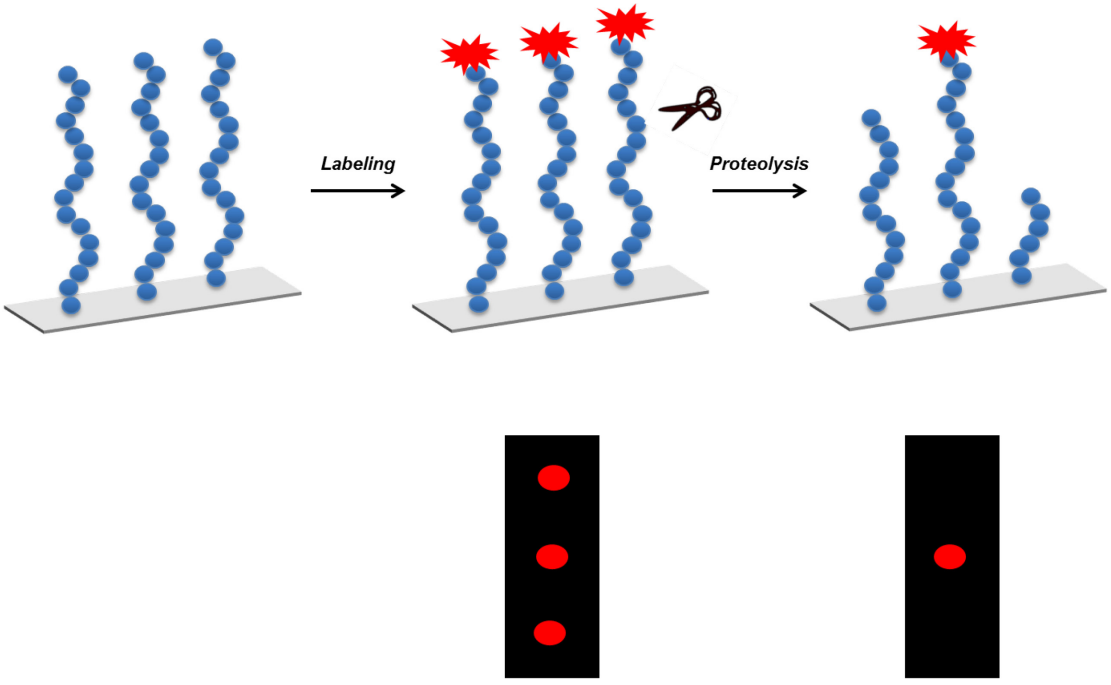

Figure 6: Schematic workflow of fluorescence labeling and proteolysis.

End-point measurements can be easily performed by using common UV/Vis- or near-infrared scanners, depending on the emission wavelength of the used dye. On-demand kinetics will be measured by the collaboration partners at *IMTEK* (University of Freiburg) in a microfluidic device.

First a model system will be developed, testing different fluorescent reagents, regarding compatibility with the synthesis process, including subsequent deprotection of the peptides. Further it will be focused on labeling efficiency and signal-to-noise ratio. In the next step proteolysis will be performed, using known enzymes, to analyze substrate specificity and sensitivity, as well as surface applicability. After validating the system, clinical specimen will be tested.

III. Results & Discussion

In this thesis the development of a high-throughput array-based enzymatic assay-system was performed, using high-density peptide microarrays (*PEPperChip™*) from *PEPperPRINT© GmbH*. In the first part of this chapter, different labeling approaches are discussed, in order to measure the enzymatic activity in a sample of interest on the array. Therefore the in-situ synthesized microarrays were directly used as delivered.

In the second part, optimizations of the surface coating and alternative polymers are discussed in terms of biocompatibility, applicability and sensitivity of the assay system. It has to be mentioned, that the standard synthesis surfaces for the laser printer-based peptide array synthesis have a format of 22 x 21 cm^2. Therefore, only reaction conditions, which could easily be up-scaled to this format, were of interest. This excludes either sensitive materials, which for example have to be held under inert gas atmosphere or have no chemical robustness or very cost-intensive reactants.

III.1. Labeling of in-situ synthesized peptide microarrays (PEPperChip™)

III.1.1. Direct labeling using fluorescent dyes

In order to develop an on-chip proteolytic assay system based on peptide microarrays, the most convenient method is to modify the peptides with a specific label, which can be read out in an on-demand or end-point measurement. The most convenient method is using fluorescent dyes, which are commercially available in various forms, depending on the coupling chemistry used and the wavelength of interest. This chapter provides an overview of the most common coupling chemistries used in peptide chemistry, together with their assets and drawbacks for the targeted assay platform.

III.1.1.1. Amino-chemistry

Because the peptides synthesized on the microarrays are oriented from C- to N-terminus, the easiest way to label them is via the N-terminal amino group, which has to be deprotected with a 50 % (v/v) piperidine / DMF solution, prior to further use. There are mainly two reaction strategies; one is to use standard *Merrifield* chemistry, by incubating the peptide array with a slightly basic mixture of a fluorescent dye with a free carboxylic group and an activation

reagent. Usually compounds of the carbodiimide family, like DCC, are used to form an O-acylisourea intermediate. Newer developments use triazoles and uronium-based coupling reagents like HOBt and HBTU to avoid racemization[64]. Figure 7 illustrates the mechanistic details.

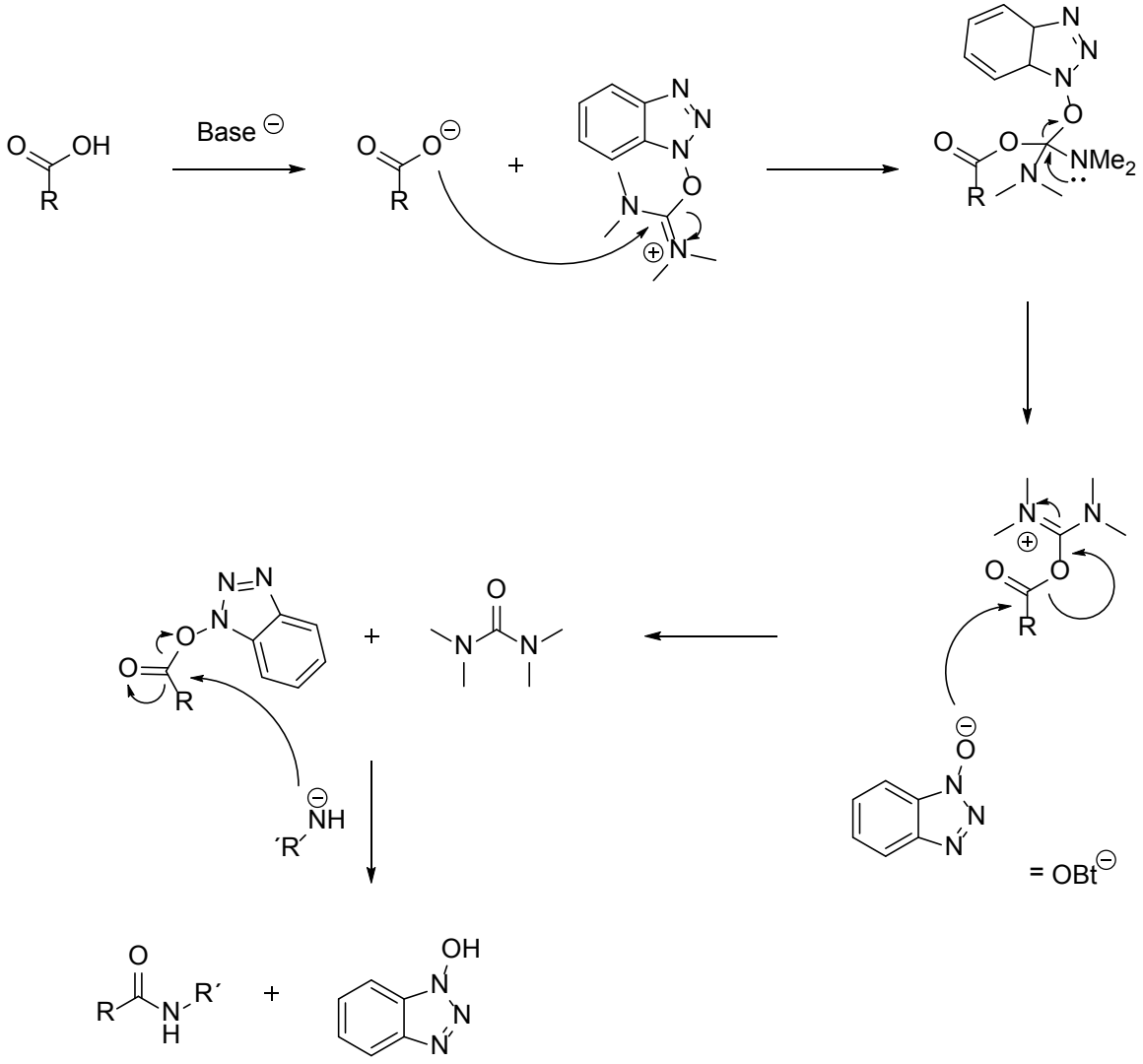

Figure 7: Coupling of a free carboxyl group to an amino group using standard *Merrifield* chemistry with HBTU and HOBt as activation reagents

In the first step the carboxyl group is deprotonated by a base. The resulting carboxylic anion can then attack the activation reagent HBTU, to form an O-acylisourea intermediate, which is replaced by HOBt, releasing N,N´-tetramethylurea. The OBt^--residue as good leaving group can finally be attacked by the amino group of the immobilized peptides, to form the labeled adduct. Another strategy is to use pre-activated compounds. A huge variety is commercially available, for example OPfp-esters, for usage in organic solvents or NHS- and sulfo-NHS-esters, which can be used in aqueous media and are therefore advantageous for biochemical reactions. Figure 8 shows the reaction schematically. The reaction mechanism

is a simple nucleophilic substitution (S_N2-reaction), with the activated ester as a good leaving group.

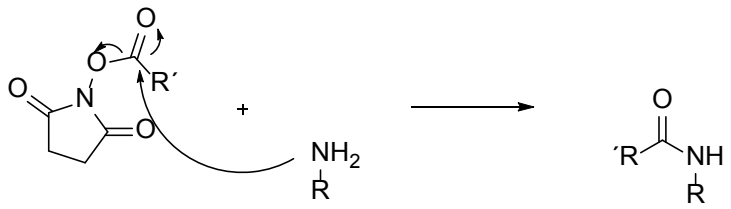

Figure 8: Mechanism of an NHS-ester activated reactant coupling to a free amino group

Prior to any enzyme incubation, the peptide side-chain protecting groups have to be removed by using a 95 % TFA solution. Because of their acid stability, fluorescent dyes of the Tetramethylrhodamine (TAMRA) family were used, namely the free acid for *Merrifield* coupling and its NHS-ester homologue for reactions in aqueous buffer. The two mentioned reaction chemistries were studied, following standard protocols.

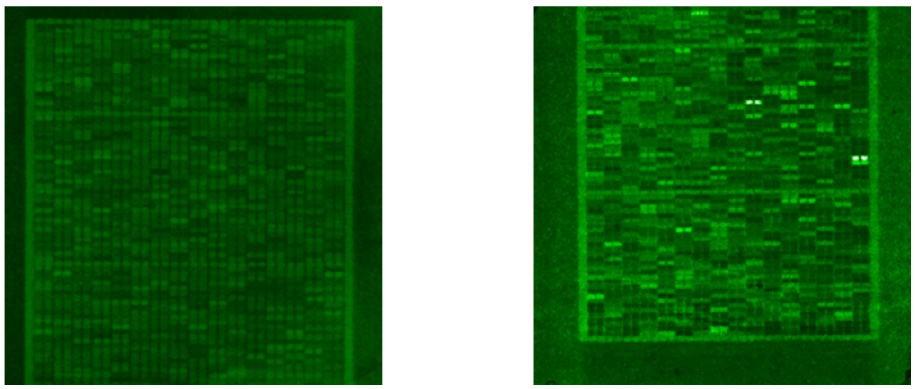

Figure 9: Peptide array N-terminal labeled with 1mM TAMRA-Lys-COOH, using HBTU/HOBt as activation reagents (left) and 0.02mM TAMRA-NHS (right). Read out was performed on the *Genepix scanner* (PMT400).

Figure 9 shows the two amino mediated labeling trials. The signal-to-noise ratio for the HBTU/HOBt coupling is with a value of 2.26 slightly better than TAMRA-NHS with 1.75 respectively. The variances in labeling efficiency could be attributed to electrostatic interactions between the charged dye molecules and the peptide backbones, if compared with the biotin labeling in chapter III.1.2.3. Highly fluorescent peptide spots tend to have a balanced number of positive and negative charged amino acid residues or a large number of nonpolar rests. Also N-terminal located glycine and serine rests seem to have a positive impact on the fluorescent intensity. On the other hand, peptide sequences containing aromatic amino acids, as tryptophan, phenylalanine tyrosine or histidine show dark spots, which can be explained due to intramolecular quenching[65]. A high number of acidic residues

resulted also in a low fluorescence intensity. However, no general trend can be observed here. The following protease incubation though, showed no cleavage of any peptides compared to the buffer control (fluorescence scan not shown). A sterical hindrance of the proteases due to the attached dye molecule can be excluded. In the dissertation of *Yepes,* it was shown that TAMRA-labeled spotted peptides are successfully cleaved on the standard PEGMA/MMA surfaces[66]. Another possibility could be cross-reactivity of the activated reagents with hydroxyl groups in the polymer, which maybe remained uncapped during the synthesis process, especially in deeper layers. Therefore, thiol chemistry, as more specific reaction chemistry, was tested below.

III.1.1.2. Labeling via maleimide activated fluorescent dyes (Thiol chemistry)

In order to avoid any side reactions, possibly occurring, when using amino chemistry, labeling via maleimide activated dyes was tested. Maleimide esters selectively couple to thiol-residues in a Michael addition (Figure 10). Therefore, the peptide content was adapted with an N-terminal cysteine in the synthesis process. Another advantage over the amino labeling is that this reaction pathway allows free choice of a fluorescent dye, because the labeling step can be performed after side-chain deprotection. This represents a crucial step because many fluorescent molecules are labile against strong acidic or basic conditions. Maleimide groups will only react with thiol groups, when working under neutral or slightly acidic pH, so the amine remains protonated and is therefore a bad nucleophile, compared to the –SH group[67]. Therefore no cross reactivity should occur.

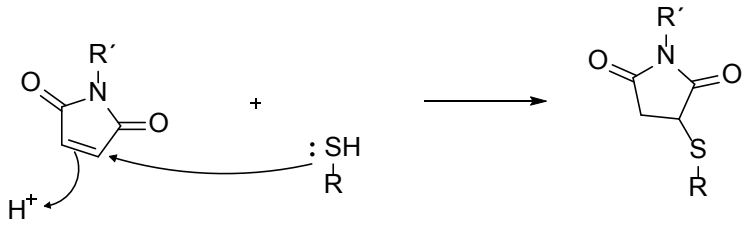

Figure 10: Mechanism of a maleimide activated compound coupling to a thiol residue (Michael addition).

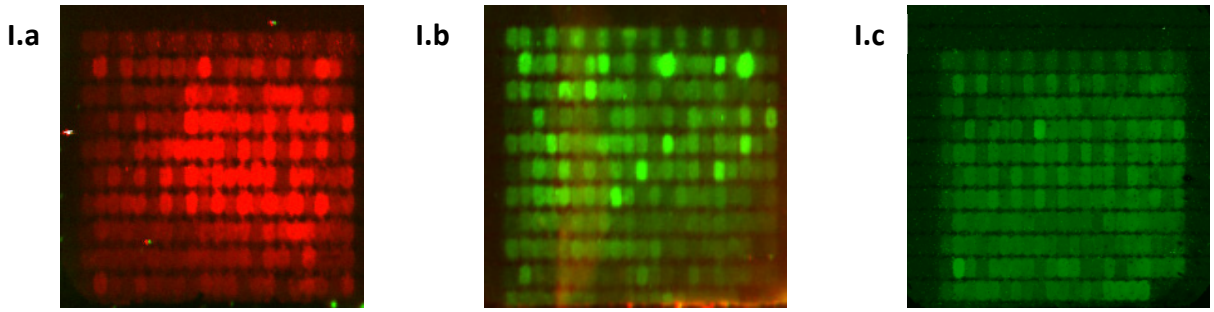

Figure 11: Comparison of maleimide dyes, I.a) 0.3µM Atto680-Mal; I.b) 0.3µM Dylight800-Mal and I.c) 0.7µM TAMRA-Mal. Read out was performed on the *Odyssey scanner* for near-infrared dyes (Atto, intensity 4 and Dylight, intensity 7) and *GenePix scanner* for TAMRA (PMT400).

The free electron pair of the sulfur atom can undergo a nucleophilic addition to the double bond of the maleimide ring. The resulting carbanion is stabilized by the –M effect from the keto groups and can finally react with a proton in solution to form the saturated product. For the maleimide based peptide labeling three fluorescent dyes, commonly used in our lab, were tested in different concentrations. Prior to dye incubation, the peptides were fully deprotected, following standard protocols. Like the NHS couplings, the reactions can be performed in aqueous media. As depicted in Figure 11, much less reagent for labeling is necessary to yield similar fluorescence intensities, compared to the amino coupling, about 1500 fold for TAMRA and 3500 fold for the infrared dyes respectively. The overall labeling homogeneity of the infrared dyes is lower than for TAMRA. Besides the possible quenching effects, mentioned before, steric hindrance caused by their around two fold higher molecular weight, could also contribute. The signal-to-noise ratio on the other hand is with 6.06 for Atto680-Mal and 13.71 for Dylight800-Mal better than for TAMRA-Mal with 3.27, which indicates again cross-reactivity of dye molecules. Because of the, in theory, high specificity of the thiol-maleimide reaction, another explanation could be non-specific adsorption to the surface polymer and/or peptide backbones, due to hydrophobic and/or electrostatic interactions. Furthermore, no proteolytic cleavage of the peptide content could be observed either. To further optimize the labeling specificity and to check, if it is a matter of non-specific adsorption, alternative reaction chemistry was introduced below.

III.1.1.3. Click chemistry

In order to avoid non-specific reactions of the labeling reagent with any functional group, which could be left after production, another common coupling strategy, the so called click chemistry was tested. This labeling approach is based on a biorthogonal reaction chemistry between both an alkyne or phosphine residue and an azido group under mild aqueous, catalyst-free conditions, without possible side reactions because of the limited number of

reaction partners of the azido group[68]. For the labeling, the peptide microarrays were N-terminally modified with β-azido-alanine out of solution, following standard *Merrifield* chemistry and the subsequent orthogonal deprotection steps. Labeling was performed with a Dylight550-phosphine dye via *Staudinger ligation*, following the manufacturers' protocols.

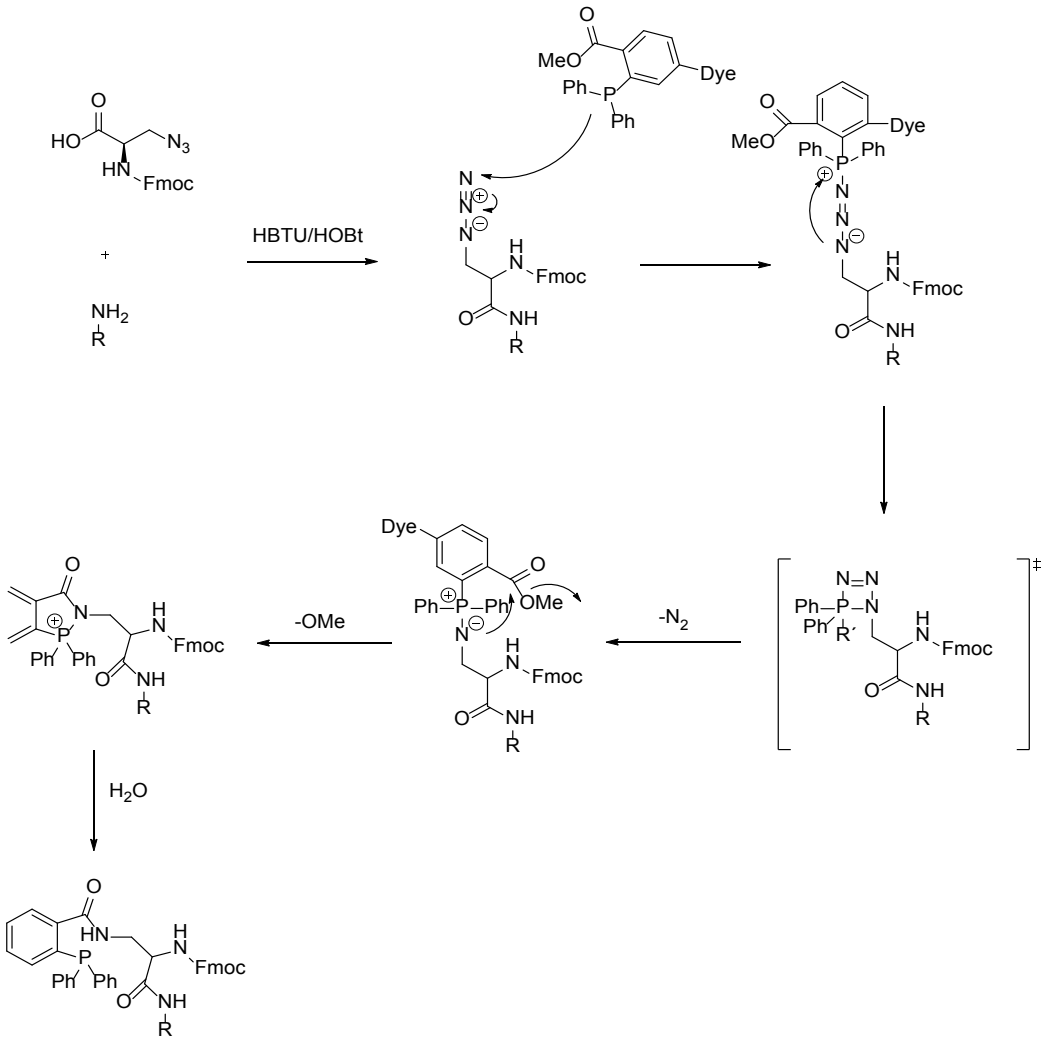

Figure 12: Mechanistic details of the *Staudinger ligation* using a phosphine modified fluorescent dye and an azido residue.

As depicted in Figure 12, the first reaction step of the phosphine coupling is an electrophilic addition of the free electron pair from the phosphorus to the electropositive nitrogen of the azido residue, followed by an aza-ylide transition state. The release of dinitrogen leads to an intramolecular rearrangement, forming the final amide bond. Figure 13 shows the fluorescence scan after labeling with Dylight550-phosphine. The need to increase the PMT value up to 600 (scan intensity), points out the low coupling efficiency, although the labeling reagents were used in excess. Also the suboptimal signal-to-noise ratio 1.5< is a major disadvantage and results partly from the auto-fluorescence of the glass. However this result indicates a non-specific binding of the dye to the surface polymer. However it has to be taken

into account that in-solution coupling of β-azido-alanine could also lead to cross reactions with functional groups in the polymer film, as assumed for the reagents coupled via *Merrifield* chemistry (see III.1.1.1.). This makes a distinction between cross-reactivity and non-specific binding to the polymer difficult.

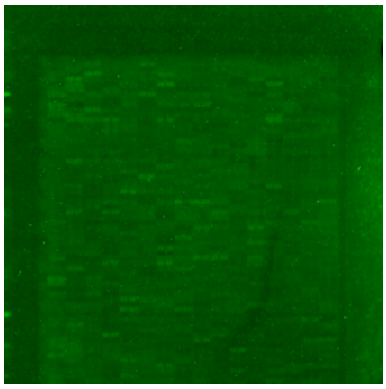

Figure 13: Peptide array N-terminally modified with 10mM Fmoc-β-azido-alanine and labeled with 10µM Dylight550-phosphine. The PMT value was increased due to the poor coupling yield; high background fluorescence hampers the analysis. Read out was performed on the *GenePix scanner* (PMT 600).

In order to test whether it is a matter of nonspecific physisorption of the fluorescent dye to the surface polymer, or covalent binding to functional groups, which have not been capped during the synthesis process, a peptide array was incubated with an azido functionalized TAMRA. Because the azido group cannot react with any functional group available on the surface, which might occur due to the synthesis process, no fluorescence should be detected.

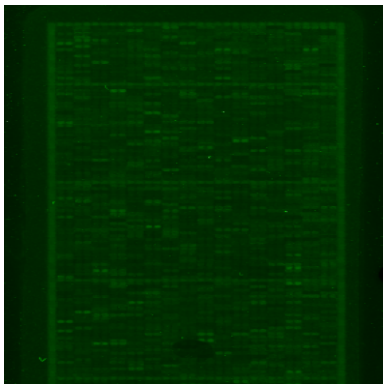

Figure 14: Fluorescence scan of a peptide array incubated with 10µM TAMRA-PEG(3)-N_3. Due to the orthogonal reaction chemistry no labeling should occur; Read out was performed on the *GenePix scanner* (PMT 500).

As Figure 14 illustrates, a fully labeled peptide pattern can be seen, which proofs the non-specific binding of the fluorescent dye to the PEGMA/MMA film, which presumably can be attributed to hydrophobic and/or electrostatic interactions. Experiments using TAMRA-COOH without any activation reagents showed similar results. Especially the high proportion

adsorbing to the peptide spots could be explained with the remains of silica and other matrix components of the micro particles, deposited onto the solid support during peptide synthesis.

III.1.1.4. Labeling via fluorescein arsenical hairpin binder ethane dithiol

Over the past few years the green fluorescent protein (GFP) or similar genetically encoded proteins, have become a very popular method to label proteins[69]. Unfortunately such a proteinogenic label cannot be used when working with an enzymatic assay system, because the label itself would be digested. In order to solve the problems occurring with the large protein sizes, metal chelating agents were designed, binding specifically to a small peptide motif. The fluorescein arsenical hairpin binder represents such a reactant, binding selectively to a tetra cysteine motif *CCXXCC* as illustrated in Figure 15, where *X* stands for a various amino acid[70]. This small binding site can easily be implemented into the peptide sequences, synthesized on the peptide microarrays and can therefore be used for a specific labeling of the peptide content prior to enzyme incubation. Interestingly, when not bound to its binding motif, the arsenic compound remains non fluorescent, so even if it adsorbs nonspecifically to the polymer surface, no fluorescent signal should be detected. Figure 16 shows the labeling of a peptide content, where each peptide bears a tetra cysteine motif at various locations within the sequence, except the first row and the left column, which represent a *FLAG/HA-epitope* control frame. For the first test the same concentration of labeling compound was used, as found in commercially available labeling kits, for example from *life technologies*. Due to the high PMT value and long incubation time needed, an excess of FlAsH-EDT_2 was finally used together with DTT as reducing agent to avoid the formation of disulfide bridges between the cysteine residues, which would inhibit the complexation. This resulted in higher fluorescence intensities with signal-to-noise ratios of 1.26 and 1.27 respectively, which is possibly caused by auto-fluorescence of the glass itself. However the resulting pattern shows a lack in specificity of the arsenic compound. In Table 2 exemplary peptide sequences are pointed out.

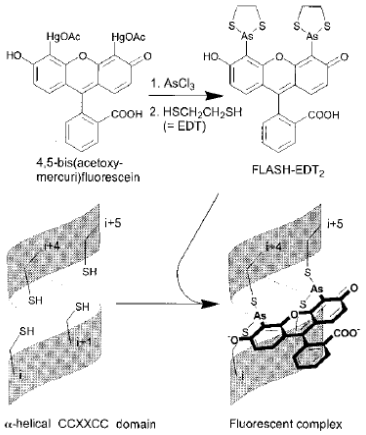

Figure 12: Synthesis of FlAsH-EDT$_2$ and proposed structure of its complex with a α-helical tetra cysteine containing peptide/protein domain [6]

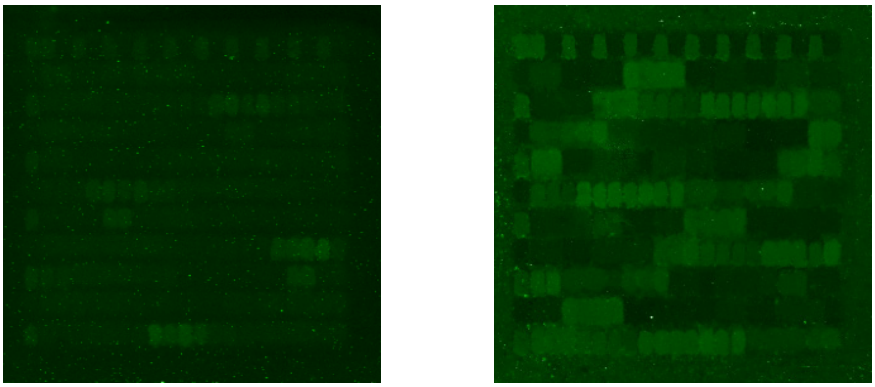

Figure 13: Peptide array labeled with 0.2mM FlAsH-EDT$_2$ overnight (left) and 7.5mM FlAsH-EDT$_2$ + 0.1M DTT as reducing agent over 2h (right). Readout was performed on the *GenePix scanner* (PMT600).

Sequence	Average fluorescence intensity [%]
H_2N-YPYDVBDYAGSGSGS (*HA*-Tag)	44
H_2N-DYBDDDDBGSGSGSG (*FLAG*-Tag)	50
H_2N-QSYDSBDYSD**CCXXCC** (HA-rel-Tag)	67
H_2N-**CCXXCC**DYBDDDDBGS	28
H_2N-**CCXXCC**QSYDSBDYGS	4
H_2N-**CCXXCC**YPYDVBDYAG	0

Table 2: Exemplary peptide sequences labeled with FlAsH-EDT$_2$ with their corresponding average intensity values. B stands for the amino acids K and R; X stands for a various amino acid.

The highest fluorescence intensities were achieved with a combined sequence of *HA-rel-Tag* (*HA* - Human serum albumin) attached to the C-terminal tetra cysteine motif. The *FLAG-Tag* sequence also yielded high intensities both combined with other sequences or as stand-

[6] Griffin, B. a, Adams, S. R. & Tsien, R. Y. Specific covalent labeling of recombinant protein molecules inside live cells. *Science* **281,** 269–272 (1998).

alone motif, whereas the *HA-Tag* shows fluorescence only when bound to other domains than the tetra cysteine sequence. If taken N-terminally, the tetra cysteine motif showed only low intensities; the best results were yielded in combination with the *FLAG-Tag*. For all tested sequences replacing amino acid B with an alanine lead to no fluorescence, which indicates the necessity of the amino group for complexing the arsenic atoms. It seems that aspartic acid, tyrosine and also amino residues are able to complex the arsenic centers of the dye when they take the right orientation to function as π-donor. For binding the tetra cysteine motif, the right location in the peptide sequence as well as the surrounding domains seem to be critical to form a proper α-helical orientation. For the desired assay system, the label needs to be attached N-terminal, so that an enzymatic cleavage of the subjacent peptide sequence can be assured. Preliminary experiments showed that the arsenic compound lacks in binding its tag specifically when it is located N-terminally. Due to this incompatibility, FlAsH-EDT_2 was not pursued further.

III.1.1.5. Short summary and conclusion

In the first part of this chapter it has been shown that labeling via NHS-ester activated fluorescent dyes, as well as standard *Merrifield* chemistry, lead to similar results, regarding fluorescence intensity and signal-to-noise-ratio. However the NHS-ester turned out to be advantageous, due to the lower amount of reagent needed and the possibility to use aqueous buffer conditions instead of organic solvents. Because of the subsequent deprotection step with a TFA solution, acid stable fluorescent dyes of the tetramethylrhodamine family (TAMRA) were chosen. The peptide sequence composition in each spot turned out to highly influence the resulting fluorescence intensity, in terms of polarity, charge and quenching. However, a successful proteolysis after labeling could not be achieved. Sterical issues were excluded, due to the positive cleavage of TAMRA-modified peptides in spotting experiments of *Yepes*. The possible cross-reactivity with functional groups, which could have remained uncapped during the synthesis process, especially in deeper polymer layers, lead to the introduction of a more specific alternative labeling strategy. Reactions via maleimide activated compounds and cysteine residues are highly specific, as long as the reaction parameters, especially the pH value, are controlled. Another advantage is the possibility to use not only acid stable, but the whole spread of fluorescent dyes available because the side chain deprotection can be performed before labeling and not afterwards. However, labeling via maleimide activated fluorescent dyes showed no significant increase in specificity. To test if it is a matter of cross-reactivity with remaining functional groups in the polymer film or rather a problem of non-specific adsorption, click

chemistry was used. Incubation of unmodified peptide content with an azido-TAMRA and also its free acid without activation reagents, revealed non-specific binding of the dye to the polymer surface and especially to the peptide spots. In the dissertation of *Münster* it was found that due to the melting process of the micro-particles, the silica based matrix forms a porous landscape on top of the polymer film. Even with stringent washing there might remain rests of silica or other matrix components, causing unwanted side effects, due to for example hydrophobic interactions, leading to the observed unspecific binding of labeling molecules.[71] This effect was mainly observed when performing reactions from solution. Further it seems that in-solution reactions allow the diffusion of reactants deep into the polymer film, whereas using the in-situ method only a local restricted penetration because of the gel-like pillow, which is formed while melting the micro-particles, is achieved. Unfortunately it is not possible to implement fluorescent dyes into the micro-particle based synthesis, due to technical issues. To overcome this problem a fluorescein based arsenic compound, which shows only fluorescence, when complexed with its binding motif, was tested. However transferring this method to peptide microarrays showed a lack in specificity, most likely due to the false orientation of the peptides relative to the arsenic centers of the fluorescent dye. Checking for proteolysis after labeling with a fluorescent dye (no matter which labeling chemistry was used before), using standard enzymes, as proteinase k and trypsin, showed no decrease in signal intensity at all. It can be assumed, that the non-specific interactions of dye molecules with the polymer surface and remnants of the micro-particle matrix within the peptide spots, present an overlap, so that the actual decrease in fluorescence intensity due to proteolysis cannot be detected. In order to check if on-chip proteolysis is working in general with the PEPperChip™ system, an indirect labeling system with end-point measurement was further used, to avoid chemical modification of the in-situ synthesized peptides but to use them right after the synthesis.

III.1.2. Indirect labeling techniques

III.1.2.1. Labeling via FLAG/HA antibody epitope tags

A well-established technique in biochemistry used for purification, Western blot analysis and many more, is the fusion of an epitope tag to a protein of interest. For example a poly histidine sequence (His-tag) can be used for affinity purification due to its metal chelating properties. Other epitopes like the *FLAG-* and *HA-tag* are frequently used together with their specific *anti-FLAG* and *anti-HA* antibodies.[72] This system can also be implemented on a

peptide array. In order to test if proteases are active on the PEPperChip™ arrays, the peptide content was adapted with an *FLAG*-, *HA*- and *HA-related tag* respectively, listed in Table 3.

	Sequence	**Specific antibody**
***FLAG*-tag**	DYKDDDDK	monoclonal mouse-anti-*FLAG* M2 IgG
***HA*-tag**	YPYDVPDYAG	monoclonal mouse-anti-*HA* 12CA5 IgG
***HA*-related tag**	QSYDSKDYSD	

Table 3: List of the used tag-sequences with their specific antibodies; different to the *FLAG*-tag, the *HA* and *HA*-related sequences can be permutated without losing complete antibody specificity.

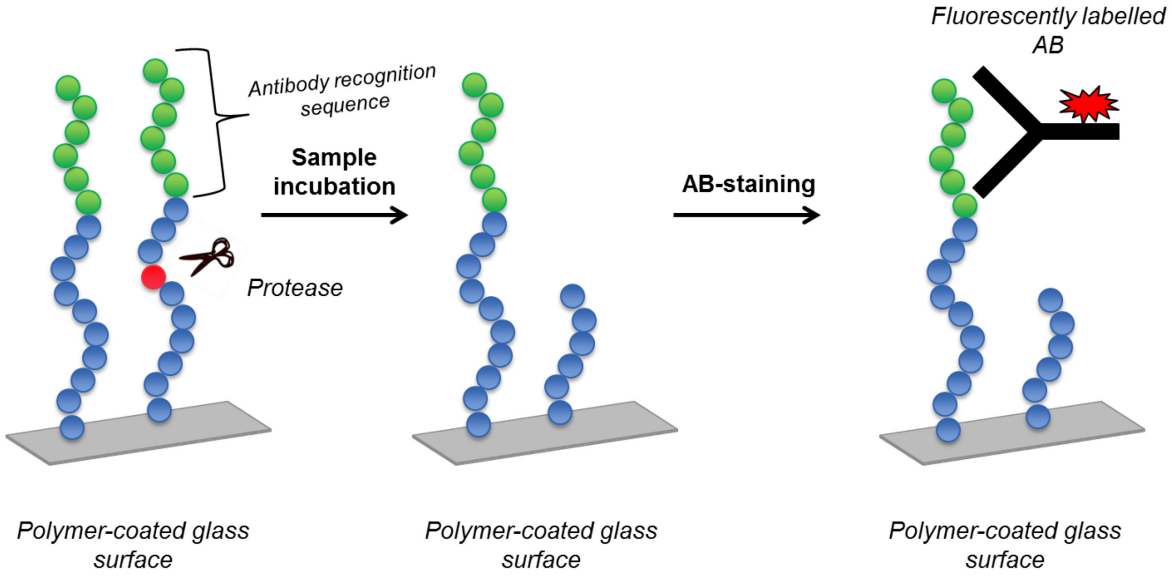

Figure 17: Schematic workflow of the *FLAG/HA*-assay system.

As depicted in Figure 17 the basic idea is that the fluorescently labeled *anti-FLAG* and *anti-HA* antibodies will bind only to full-length peptides, where the epitope sequence is complete. When the peptide sequence is cleaved by a protease, the antibody recognition will fail and a decrease in fluorescence intensity for this peptide spot can be measured compared to the buffer control. The in-situ synthesized arrays were used as delivered without further chemical modification; the protection groups were cleaved following the corresponding protocols of the manufacturer and the array then blocked with a 2% (m/v) PVP-TBS-T solution, to avoid nonspecific adsorption of proteases to the polymer surface. PVP as non-proteinogenic compound was used because it will not interfere with the enzyme incubation. After proteolysis the array was again blocked, this time using Rockland buffer©; as standard proteinogenic blocking agent used in the lab, it reduces background fluorescence due to non-specific binding of antibodies to the polymer surface.

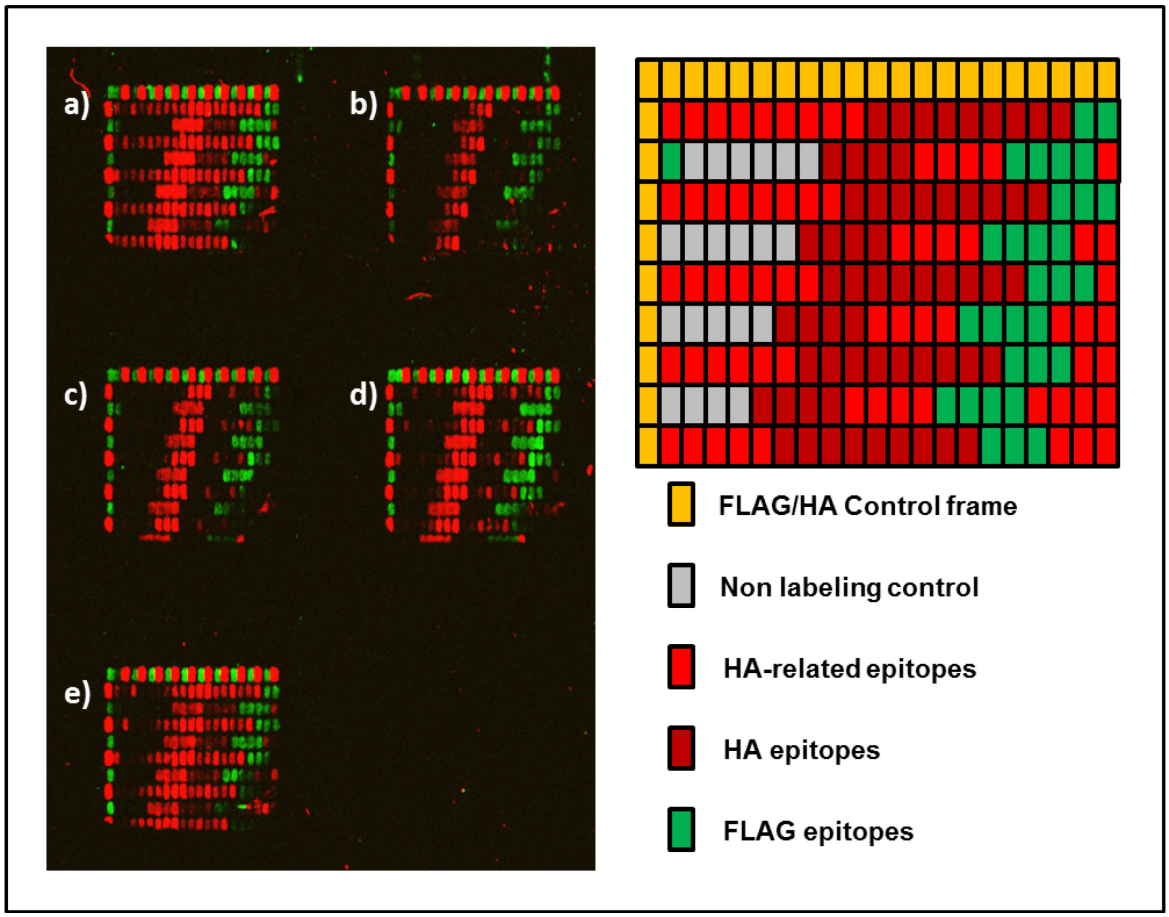

Figure 18: Peptide array (17meres) with *FLAG*-, *HA*- & *HA*-related sequences, stained with their specific antibodies after protease incubation length (the 10mere epitopes were elongated with a repetitive GS-sequence); a) buffer control, b) proteinase k, c) trypsin, d) chymotrypsin, e) elastase. Overall enzyme concentration was 5µM, 2h incubation time at 37°C; antibody staining was performed with a 1:1000 dilution out of a 10mg/ml stock solution; Read out was performed on the *Odyssey scanner* for near-infrared dyes (intensity 7).

Figure 18 shows the fluorescence scan after enzyme incubation and antibody staining with the corresponding peptide map. For each peptide spot five replicates were printed. For data quantification the decrease in fluorescence intensity of the enzyme incubated subarrays was compared with the buffer control. To reduce the failure of diverse spot morphologies, the average over identical sequence replicates was taken. The intensity variances in the buffer control can be explained due to different binding forces between the antibody and its epitope when the sequence is slightly substituted with other amino acid residues.

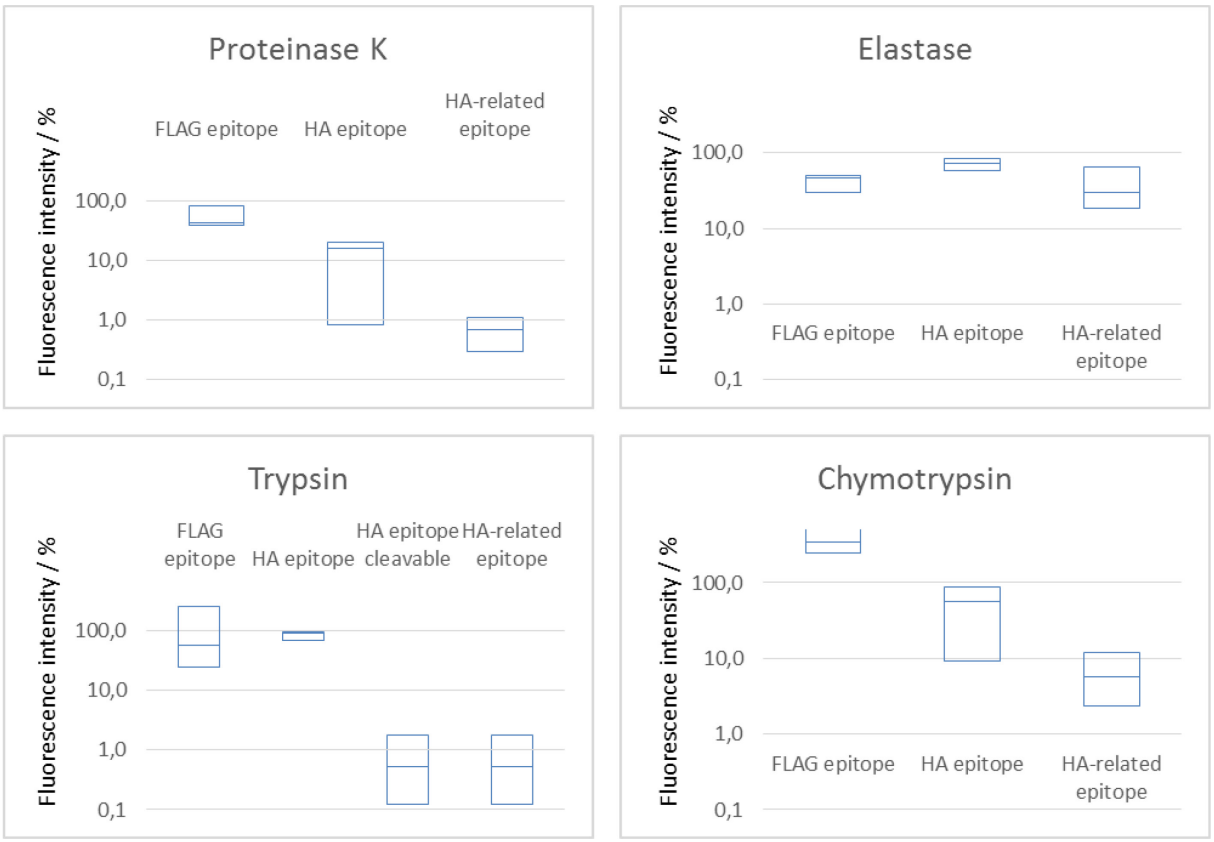

Figure 19: Quantification of the fluorescence scan (Figure 12) after 5µM enzyme incubation at 37°C for 2h. For analysis the average over 5 identical peptide spots was taken, the box plots show the minimum and maximum possible decrease in fluorescence intensity due to proteolytic cleavage including the outliers, proteinase k and trypsin were scaled logarithmically for a better overview; Analysis was performed using the PepSlideAnalyzer Software; the boxplots show the range between minimum and maximum cleavage efficiency and median value.

As depicted in Figure 19, the best cleavage efficiencies were obtained for the *HA*-related epitope, down to almost zero percent fluorescence intensity due to the various cleavage sites in the epitope sequence. Trypsin, cleaving specifically after lysine and arginine residues, shows the best results when comparing the *HA-tag* which does not bear a tryptic cleavage site with its cleavable analogues. Chymotrypsin is active against aromatic amino acid side chains but shows a lower significance against the *HA*-epitope, similar to proteinase k with its unspecific endo- and exo-proteolytic properties. Elastase showed the lowest cleavage activities in this set of proteases. However a low cleavage of the *FLAG*-epitope was obtained only with trypsin and elastase maybe due to its higher content of acidic amino acids in the sequence or the orientation relative to the active centers of the enzymes. As illustrated in Figure 20, the control frame sequences, although consisting of *FLAG*- and *HA-tags*, were not cleaved at all. One explanation could be the short peptide length, only 8meres compared to the full-length peptide content with its 17-20meres. Therefore it is harder for the enzymes to reach the cleavage sites.

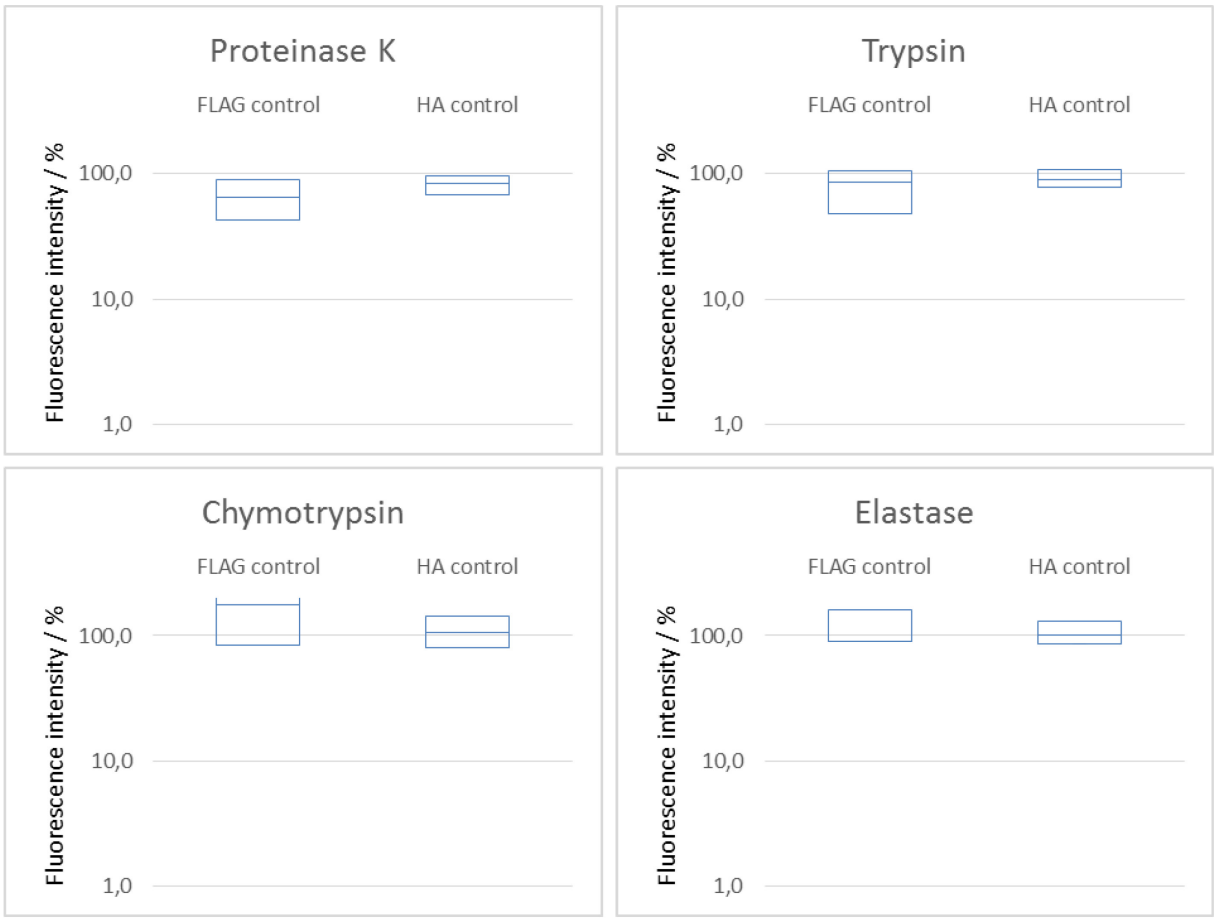

Figure 20: Quantification of the fluorescence scan (Figure 18) control frame after 5µM enzyme incubation at 37°C for 2h. The control sequences were directly synthesized on the polymer without elongation and N-terminally acetylated.

After those results further experiments using trypsin and endoproteinase asp-N, as two very specific proteases, latter cleaving after aspartic acid residues, were done to check for reproducibility and to minimize the extent of outliers due to protease specificity. Furthermore, the enzyme incubation time was extended to look for maximally possible cleavage efficiency. Figure 21 shows the obtained fluorescence scan for two different enzyme concentrations after overnight incubation. Besides the *FLAG*-epitope several *HA*- and *HA-related tags* with and without tryptic cleavage sites were used. The 10mere epitopes were elongated using a repetitive GS-sequence like before and substituted along the full peptide sequence from N- to C terminus. The quantification data for trypsin in Figure 22 show that for an overnight incubation even for lower enzyme concentration almost the same results can be obtained as for higher concentration. The proportionate cleavage of the *HA*-tag which does not bear a tryptic cleavage site can be attributed to chymotryptic contamination of the used trypsin. This time, the *FLAG*-epitope was nicely cleaved.

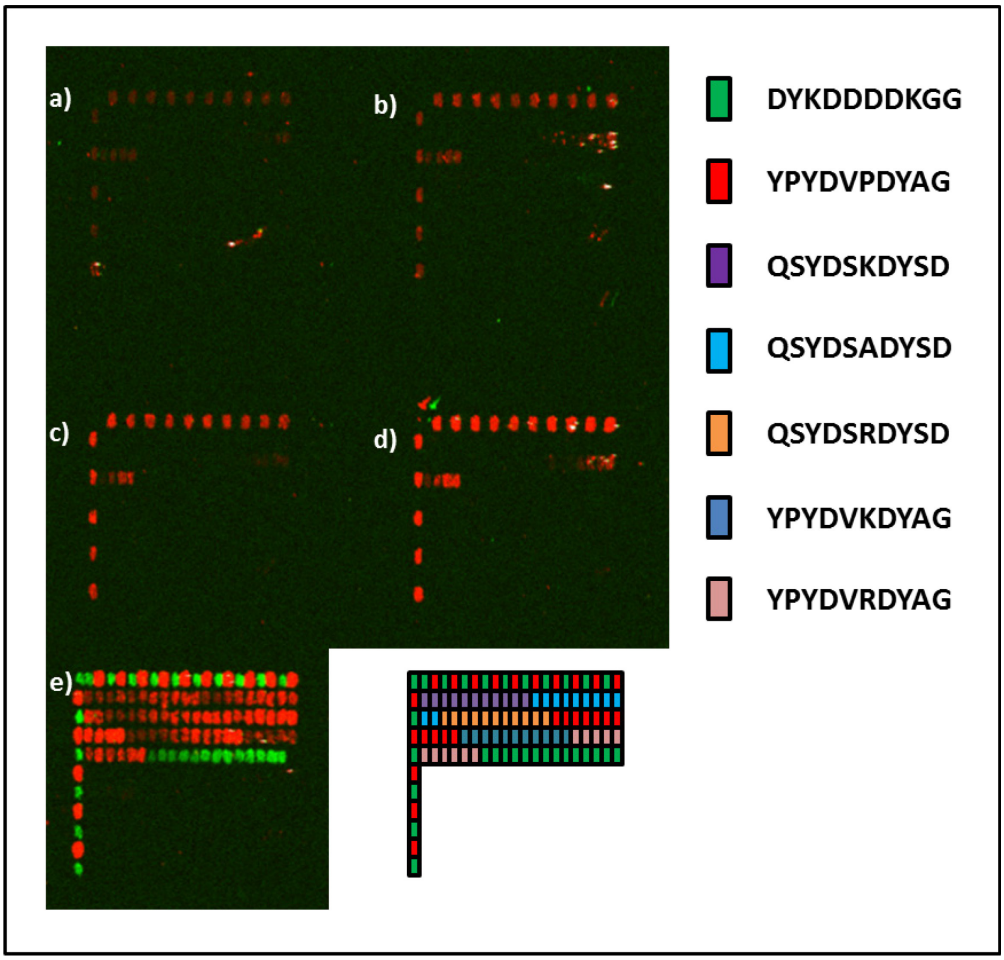

Figure 21: Peptide array (17meres) with various *FLAG*-, *HA*- & *HA*-related sequences as depicted in the legend, stained with their specific antibodies after protease incubation; the epitope sequences were substituted along the full peptide length (the 10mere epitopes were elongated with a repetitive GS-sequence). a) 125nM asp-N, b) 62.5nM asp-N, c) 5µM trypsin, d) 2.5µM trypsin, e) buffer control. Overnight incubation at 37°C; antibody staining was performed with a 1:1000 dilution out of a 10mg/ml stock solution; Read out was performed on the *Odyssey scanner* for near-infrared dyes (intensity 7).

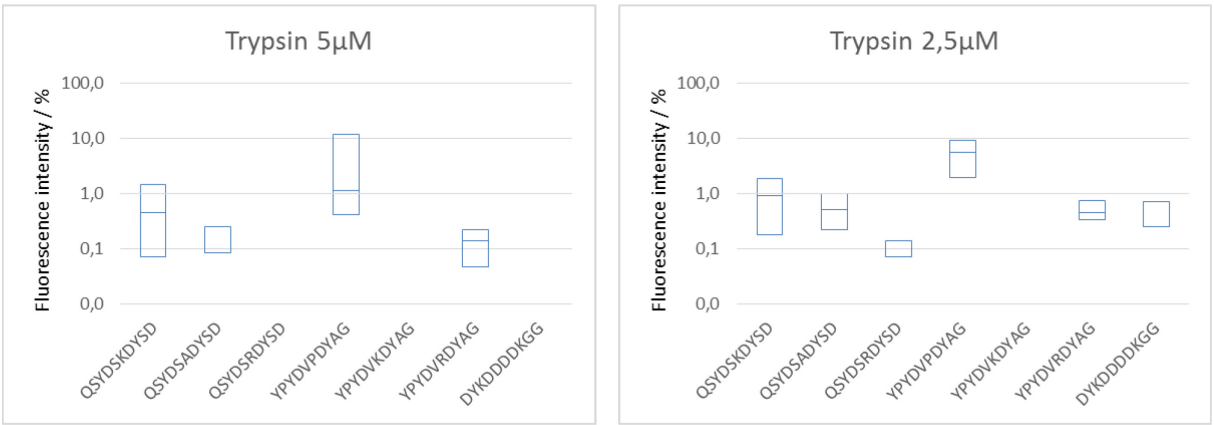

Figure 22: Quantification of the fluorescence scan (Figure 16) after trypsin incubation overnight at 37°C. For analysis the average over identical epitope sequences was taken; for sequences which were completely cleaved, no boxplot is shown. Analysis was performed using the PepSlideAnalyzer Software.

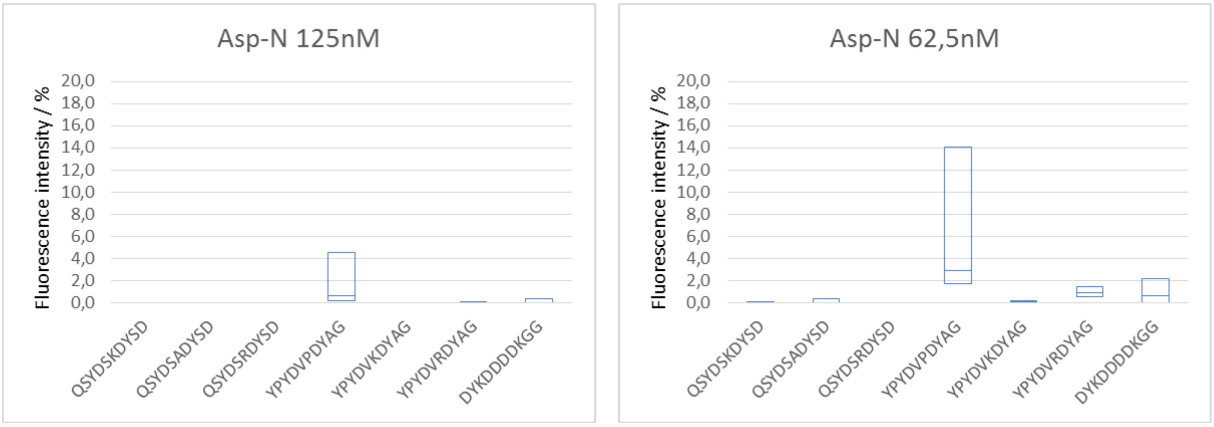

Figure 23: Quantification of the fluorescence scan (Figure 16) after asp-N incubation overnight at 37°C. For analysis the average over identical epitope sequences was taken; for sequences which were completely cleaved, no boxplot is shown. Analysis was performed using the PepSlideAnalyzer Software.

Asp-N as highly specific sequencing protease yields an overall very good cleavage of all peptides bearing an aspartic acid side chain. As a next step the concentration dependency of trypsin for a fixed enzyme incubation time of two hours was tested, to evaluate the achievable sensitivity of this system. An incubation time of two hours was chosen because it represents a reasonable duration to address a sufficient cleavage.

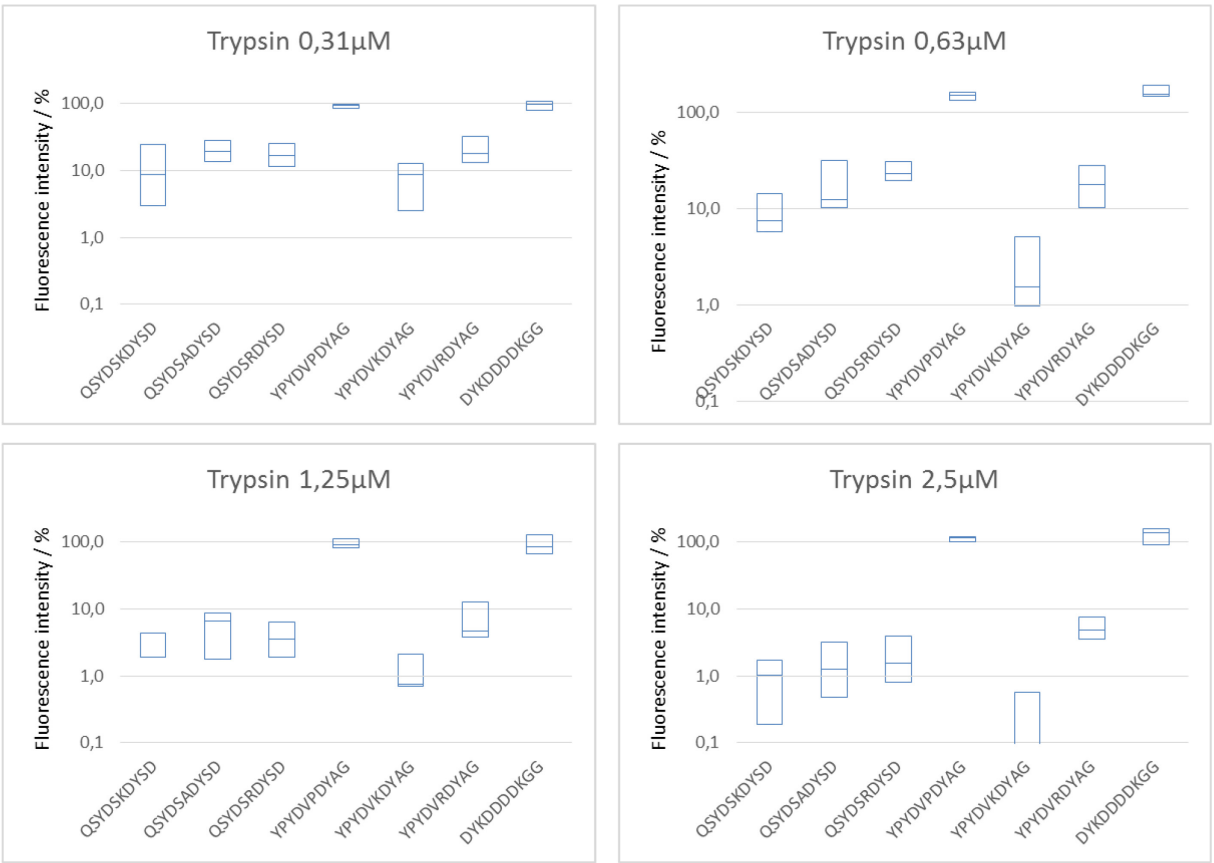

Figure 24: Quantification data of the concentration dependency of trypsin after 2h incubation at 37°C (fluorescence scan not shown). Concentrations below 0.3µM showed no significant cleavage after incubation time; for analysis the average over identical epitope sequences was taken; analysis was performed using the PepSlideAnalyzer Software.

As depicted in Figure 24, good cleavage efficiencies could be obtained with trypsin concentrations down to 0.31µM; all subordinate values were insufficient for the used incubation time (data not shown here). Finally a minimum concentration of 1.25µM showed the best results with a cleavage below 10% fluorescence intensity. However, also the cleavage of the epitope sequence *QSYDSADYSD*, without any tryptic cleavage site, was observed, likely due to chymotryptic contamination, which is caused by the production process of the used trypsin. Further the *FLAG-epitope* in this production batch remained uncleaved again which indicates a batch to batch variance.

In summary, it was shown that proteolytic cleavage of in-situ synthesized peptides on the used peptide microarrays is possible in principle. With trypsin and asp-N, as very specific proteases, the most promising results could be obtained; only the *FLAG* sequence showed batch to batch variation and no reproducible cleavage. Since the used antibody recognition sites represent a complex peptide sequence which would lead to false positive cleavage pattern in the further assay system when working with clinical specimen because it cannot be distinguished between cleavage of the epitope or the actual peptide sequence below, an alternative labeling system has to be found.

III.1.2.2. Using acetyl-lysine as antibody recognition tag

When it comes to antibody epitopes, normally a sequence of at least six amino acid residues is needed for specific binding. In 1989, *Hebbes et al.* produced an antibody which is specifically directed against a single modified amino acid residue, the ε-*N*-acetyl lysine.[73] Since this building block has been introduced as toner particle in the in-situ synthesis at *PEPperPRINT*©, it is possible to check for its suitability as non-cleavable peptide label. Therefore, the used peptide contents were adapted with an N-terminal Fmoc-ε-*N*-acetyl lysine. Prior to antibody staining the protection groups were cleaved and the slides blocked with TBS-T containing 2% PVP, to avoid non-specific binding. Afterwards the array was first incubated with the primary antibody against ε-*N*-acetyl lysine, followed by the secondary goat-anti-rabbit IgG (H+L) Dylight™680 conjugated antibody for the actual staining. The antibodies were used in different concentrations to identify the best dilution. A 1:20000 for the primary and a 1:5000 dilution for the secondary antibody yielded the best spot intensities, as depicted in Figure 25. However the signal to noise ratio turned out to be way too high for a proper analysis. Despite of that, further experiments revealed specificity problems of the used anti-acetyl lysine antibody. Peptide sequences with basic amino acid residues next to the label for example showed no binding of the antibody compared to others.

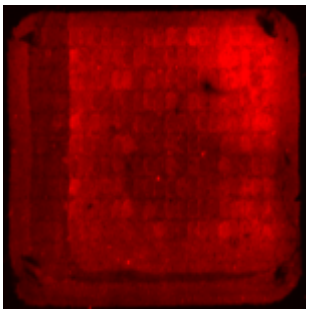

Figure 25: Peptide array (17meres) with N-terminal Ac-Lys-residues, stained with anti-MEY-ac OVA as primary and goat-anti-rabbit IgG (H+L) Dylight^{TM}680 conjugated as secondary antibody. Antibody staining was performed with a 1:20000 (primary) & 1:5000 (secondary) dilution out of a 10mg/ml stock solution, 60min & 30min respectively; Read out was performed on the *Odyssey scanner* for near-infrared dyes (intensity 7).

The obtained results lead to the conclusion that this alternative labeling system is not compatible with the aimed protease assay.

III.1.2.3. Labeling via biotin-streptavidin system

In order to find a labeling alternative for the established *FLAG/HA*-system, it had to be taken into account that the labeling molecule should be ideally non-proteinogenic and also small in size to reduce any possible steric hindrance. In the early 1960´s *Chaiet* and *Wolf* found that biotin, also called vitamin B_7, has a strong binding to a biomolecule named streptavidin, isolated from *streptamycetes*.[74] Biotin itself is a small bicyclic compound found as prosthetic group for carboxylases and also as histone modifying agent in the cell nucleus.[75] One streptavidin protein is able to bind four biotin molecules in a very strong and specific way. Therefore biotin was chosen as N-terminal labeling reagent which is commercially available as activated NHS-ester. For the analysis after protease incubation, a fluorescently labeled streptavidin was used. The biotinylation was carried out under standard aqueous buffer conditions, using a 2.2mM solution of biotin-X-NHS in PBS-T. Biotin-X-NHS has a six atom spacer arm to reduce steric effects.

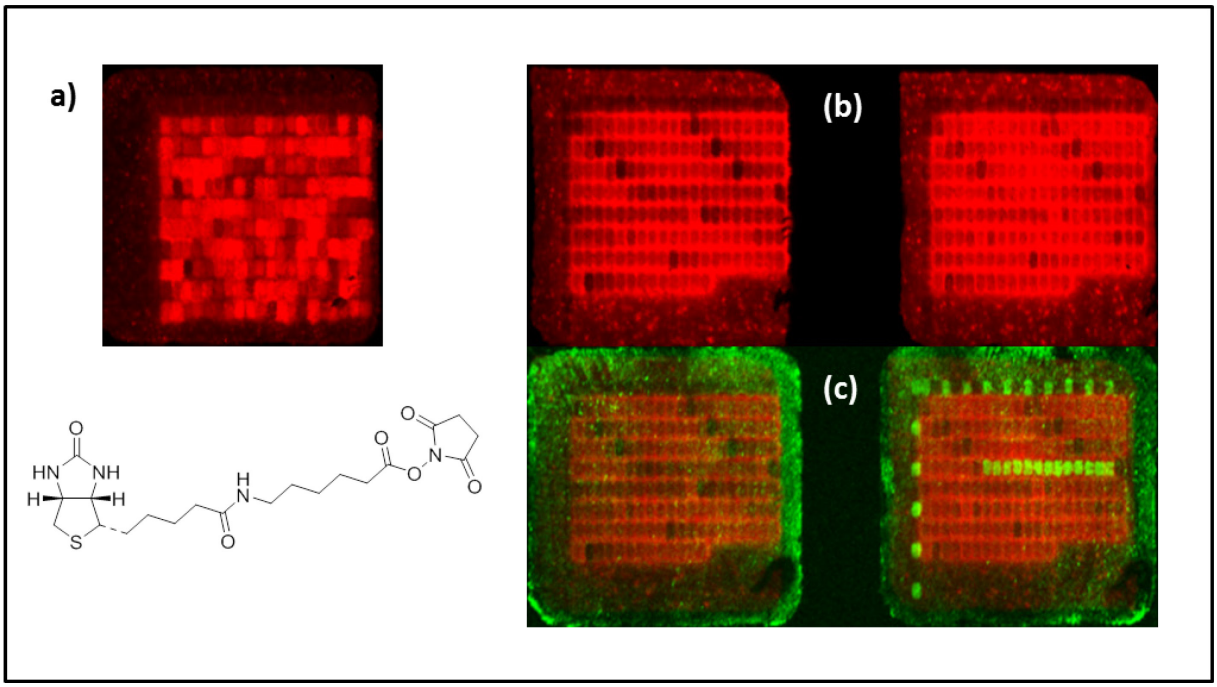

Figure 26: Peptide array (17meres) with various sequences & *FLAG/HA* control frame (top row & left column) labeled with 2.2mM biotin-X-NHS in PBS-T for 2h at room temperature. a) Streptavidin test staining & chemical structure of biotin-X-NHS; b) 2nd streptavidin test staining of buffer control (right) and 1.25µM asp-N (left); c) additional to (b) stained with anti-*FLAG*-antibody. Enzyme incubation was carried out overnight at 37°C; streptavidin staining was performed using a 1:5000 dilution out of a 10mg/ml stock solution; antibody staining was performed using a 1:1000 dilution out of a 10mg/ml stock solution; Read out was performed on the *Odyssey scanner* for near-infrared dyes (intensity 7 green channel, intensity 2 red channel).

Figure 26 shows the chemical structure of the used biotin labeling compound together with the first streptavidin test staining which indicated a good labeling efficiency and specificity (a). Also the low background interference is a plus. Further experiments however showed a lack in reproducibility as depicted in (b) where the spots show no specific labeling but the peripheral grid together with a worse background to noise ratio. When incubating with asp-N no difference in fluorescence intensity could be obtained, therefore a test staining with an anti-*FLAG* antibody was performed, shown in (c), to check for cleavage of the control frame peptides which showed a positive result. The obtained reproducibility problems seem to be similar to the ones gained with the fluorescence dye labeling. The similarity of both labeling systems lies in the in-solution coupling of the labeling compound to their specific functional groups of the peptides. To avoid the afterwards chemical modification of the peptides out of solution, a biotin toner was developed at the company *PEPperPRINT* on the basis of a biotin-OPfp-ester reagent to adapt the standard synthesis process, where the toner particles are slightly melted during the synthesis and form a gel-like pillow on top of the spots. It seems to be advantageous compared to in-solution reactions because the gel-like state allows diffusion of the reactant to the functional groups in the polymer in a very distinct area which minimizes cross-reactions in deeper polymer layers and/or unspecific physisorption.[71]

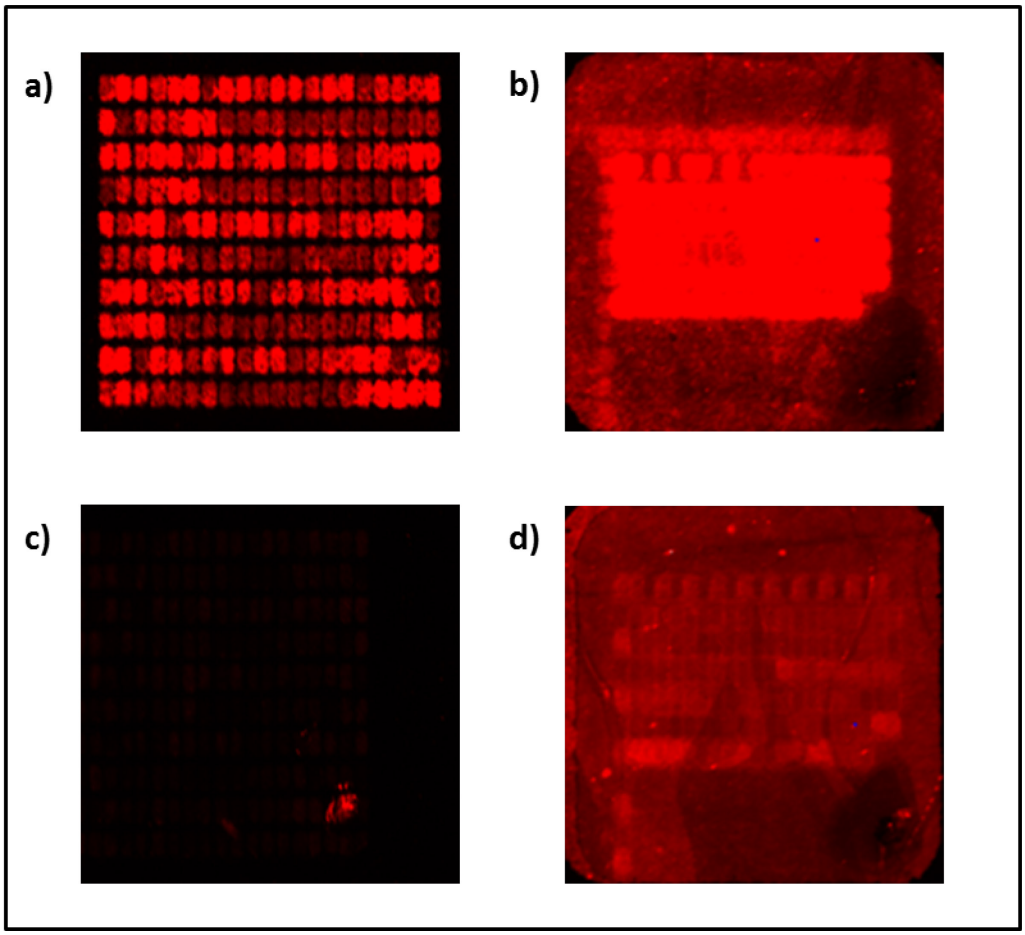

Figure 27: a) Peptide content with N-terminal printed biotin [in-situ synthesis]; b) peptide content N-terminal labeled with 2.2mM biotin-X-NHS in PBS-T for 2h at room temperature [in-solution labeling]; c) 125nM asp-N on printing-labeled array; d) 125nM asp-N on in-solution labeled array. Enzyme incubation was carried out overnight at 37°C; streptavidin staining was performed using a 1:5000 dilution out of a 10mg/ml stock solution; Read out was performed on the Odyssey scanner for near-infrared dyes (intensity 2).

Figure 27 shows the comparison between biotin labeled peptide arrays modified *in-situ* (a) and *in-solution* (b) with the corresponding proteinase k digestion (c) & (d). Obviously the *in-situ* synthesized arrays show no background fluorescence compared to the in-solution labeling which indicates a non-specific binding to the surface polymer and/or the peptides in the last case, like before when labeling with fluorescent dyes. After incubation with proteinase k the *in-situ* array shows a complete digestion of the peptide content as expected, whereas the *in-solution* array shows insufficient decrease in fluorescence, especially for the control frame and the grid of the peptide spots. This inhomogeneous pattern makes a proper analysis impossible. Further experiments were therefore based on the *in-situ* biotin labeled peptide arrays. As a next step standard protease incubation with trypsin was performed as showed in Figure 28.

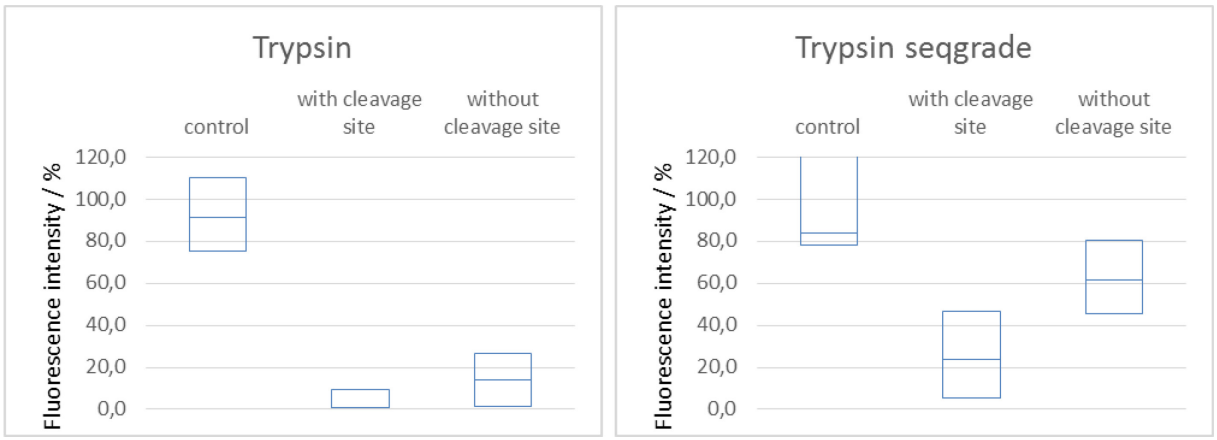

Figure 28: Quantification data of a standard peptide array after 5µM trypsin and trypsin sequence grade incubation at 37°C overnight (fluorescence scan not shown). ; For analysis the average over identical epitope sequences was taken; Analysis was performed using the PepSlideAnalyzer Software.

Here again a cleavage of both, peptides with distinct tryptic cleavage site and without, show a similar decrease in fluorescence intensity. To check if it is due to chymotryptic or other impurities of the used enzyme, trypsin in sequence grade was used. This led to a significant improvement, although still a decrease in fluorescence intensity down to around 50% for the control peptide was measured. This failure can be partly attributed to the fact that the digested spots are compared to a reference spot which is located in a different area on the microarray surface. Due to manufacturing purposes, the polymer properties within one array and the synthesis efficiency of single spots can slightly vary (leads to outliers). Further while incubating with buffers, staining solution etc. there are obviously differences because of many parameters like shaking, diffusion, protein repellency etc. that in accumulation can lead to the obtained deviations. In addition to trypsin, a protease with a more complex cleavage site was chosen to check for the potential of the present array technology. Thrombin, being an important part of the blood coagulation cascade, represents such an enzyme. It cleaves peptide sequences between arginine and glycine depending on the surrounding residues. As depicted in Figure 29, the peptide sequences from natural proteins of the coagulation system show the highest decrease in fluorescence intensity compared to the synthetic tripeptides. The control peptides show also a decrease due to some outliers (possible reasons discussed earlier in this chapter).

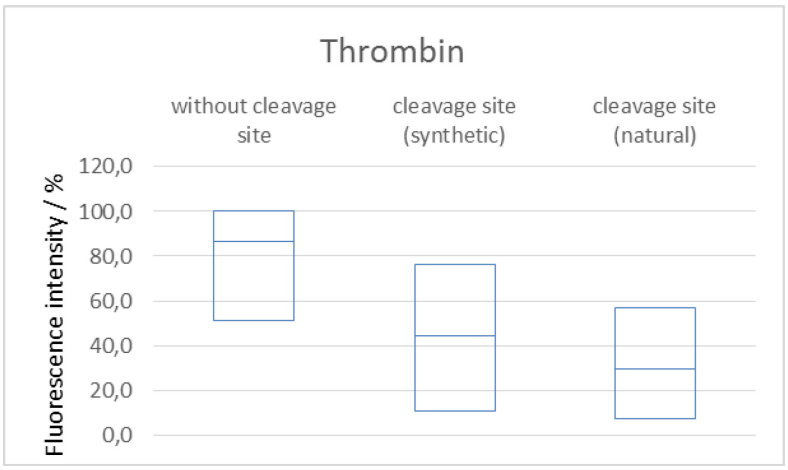

Figure 29: Quantification data of a standard peptide array after 30µM thrombin incubation at 37°C for 2h (fluorescence scan not shown). For analysis the average over identical epitope sequences was taken; Analysis was performed using the PepSlideAnalyzer Software.

III.1.2.4. Short summary and conclusion

In the second part of this chapter it has been shown that proteolytic cleavage of peptides on *in-situ* synthesized peptide microarrays is working in principle. Preliminary experiments used complex peptide epitopes (*FLAG- & HA-tag*) and their specific fluorescently labeled antibodies for detection. As such complex sequences are not suitable for an enzymatic assay system due to the possible false cleavage of the label instead of the actual peptide sequence of interest; an alternative label was needed, which does not interfere with the proteolysis. Acetyl lysine fulfills this requirement and there are specific antibodies commercially available. However the antibody binding is highly dependent on the label surrounding amino acid residues, where for example basic rests have an inhibiting influence. Further the high background to noise ratio makes an analysis very difficult and not very reliable. Despite of the antibody systems, the use of biotin as labeling tag together with its specific binding protein streptavidin, showed promising results with trypsin and thrombin as model proteases. Anyhow the preliminary proteolytic data show no complete decrease in fluorescence intensity, even when high enzyme concentrations and longer incubation times are used. There is a gap of at least 20% which could be attributed to the polymer characteristics and the loss of a degree of freedom when working on a surface based system instead of solution. In regard to optimize the system when working with more challenging proteases and finally clinical samples, the next chapter will focus on surface chemistry.

III.2. Surface chemistry

III.2.1. New polymer coating – Dextran

III.2.1.1. Background

The standard coating of a PEPperChip™ is based on a polyethylene glycol, methyl methacrylate copolymer (PEGMA/MMA) on standard glass plates, mainly following the protocol from *Stadler et al.*[76] with a film thickness of 13.5nm and a (10/90) PEGMA/MMA composition. This polymer film showed good protein repellent properties with a still sufficient wettability which is optimized by using small amounts of Tween20 as detergent. However when performing protease digestions, this coating seems to have certain limitations regarding accessibility especially for challenging enzymes like thrombin or proteases from serum samples. To address this problem another type of surface coating was tested on basis of polysaccharides which represents a biological hydrogel. Dextran turned out to be the coating material of choice because of its similar biocompatibility and protein repellency compared to PEG-based polymers. Dextran chains are not branched and remain very flexible; therefore the accessibility of peptides for proteases within the matrix should be improved.[77] Another advantage is the chemical stability and the cheap and easy synthesis process, also in regard to upscaling to production scale. Figure 30 illustrates schematically the on-chip synthesis of a dextran coating based on the protocol from *Luo et al.*[78]

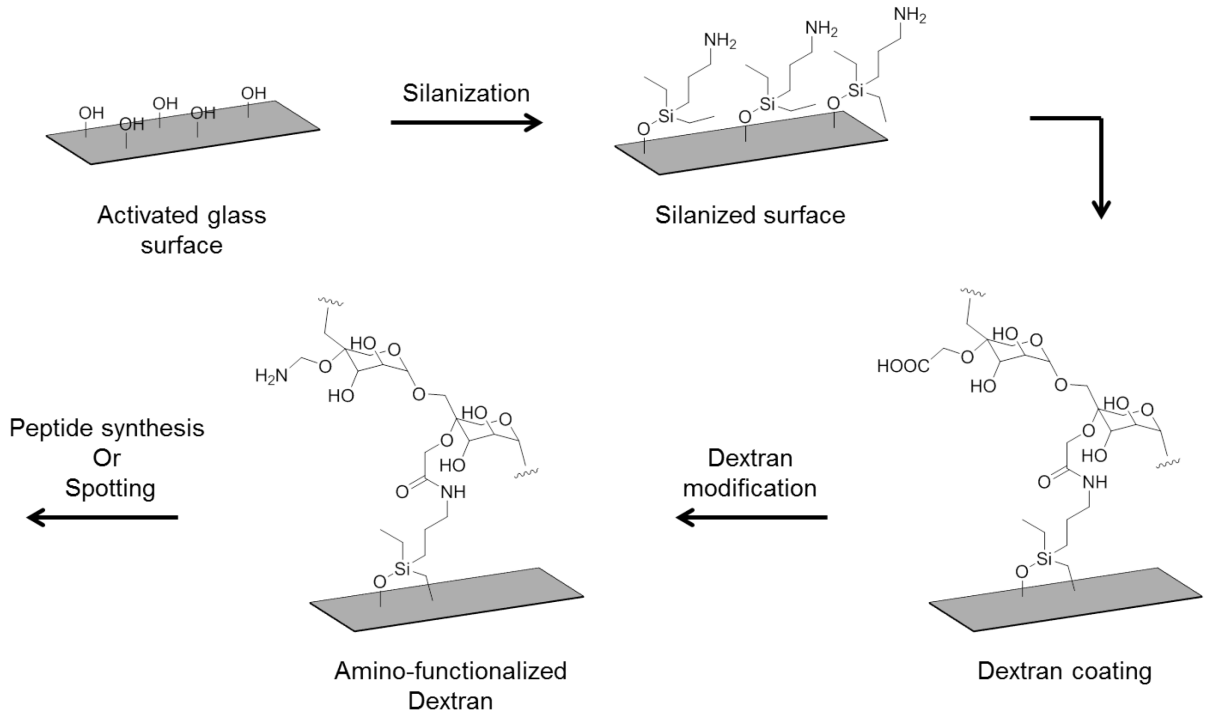

Figure 30: Schematic overview of the coating process using dextran on standard silica glass.

In the first step, standard silica glass slides were cleaned and activated by overnight incubation in a 1M KOH/^{i}PrOH solution. After washing and curing, the slides were silanized with APTES / DCM solution overnight, followed again by a curing step. The resulting amino terminated surfaces were then modified using an activated CM-dextran. Finally the dextran matrix was amino functionalized to be further used for spotting or in-situ peptide synthesis.

III.2.1.2. Test of dextran coating with spotted peptides

Figure 31 shows the polymer thicknesses after silanization and dextran modification verified via ellipsometry. Different concentrations of silane and dextran solutions were tested in order to find the optimum polymer composition.

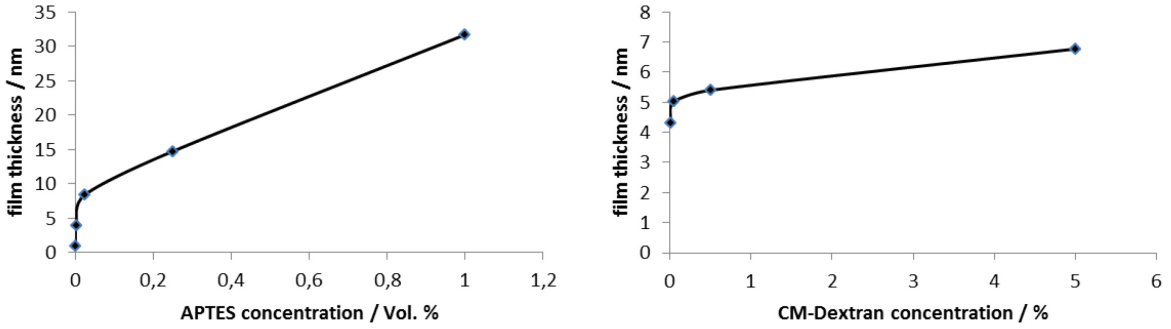

Figure 31: Characterization of silane & dextran layer; left: Variation of thickness of the silane layer with change in APTES concentration after overnight incubation on Si(100) wafer; right: Variation of thickness of the dextran layer with change in CM-Dextran concentration after overnight incubation on silanized Si(100) wafer (0.0025% APTES).

The silanization using APTES showed a linear increase in film thickness. Higher concentrations up to 2.5% led to thick multilayers of around 80-90nm which stands for about 100 layers with regard to its monomer size of 0.89nm.[79,80]. After the following dextran modification, using a 5% dextran solution, a resulting polymer thickness of 13-16nm was achieved which indicates a loss of silane layers during dextran incubation and the instability of such thick silane films. Therefore, a reduced APTES concentration (0.0025%) was used, which led to a stable 4.49nm layer, to test for the variation of thickness of the dextran layer. The dextran modification showed a rather asymptotic increase in polymer thickness up to around 7nm. A 5% dextran solution gave the best results regarding polymer stability against chemicals used in SPPS. Regarding the reproducibility of silanization, a 2.5% APTES solution was further used to ensure a proper reaction. Polymer stability was in this case the main priority whereas the polymer thickness should not interfere with its biocompatibility. For

the following spotting of N-terminally biotinylated sample peptides, the amino terminated polymer surface was functionalized by using a NHS-maleimide linker for the cysteine mediated linkage. Table 3 shows the peptide sequences used for this experimental setup. Peptides 1 and 2 represent a synthetic thrombin cleavage sequence where the enzyme cleaves after proline and arginine. The hexamer sequence was located N-terminally for peptide 1 and C-terminally for peptide 2 to check for accessibility of the enzymes. Peptide 3 represents a natural thrombin cleavable sequence from fibrinogen. All three sample peptides also contain cleavage sites for trypsin.

	Sequence
Peptide 1	Bio-**GSLVPR**GSGSGSGSGSKKGC
Peptide 2	Bio-GKKSGSGSGS**GSLVPR**GSGC
Peptide 3	Bio-**LSNNAIGPRSFSQNSRHP**GC
Control	Bio-GSGSGSGSGSGSGSGSGSGC

Table 3: Set of spotted peptides.

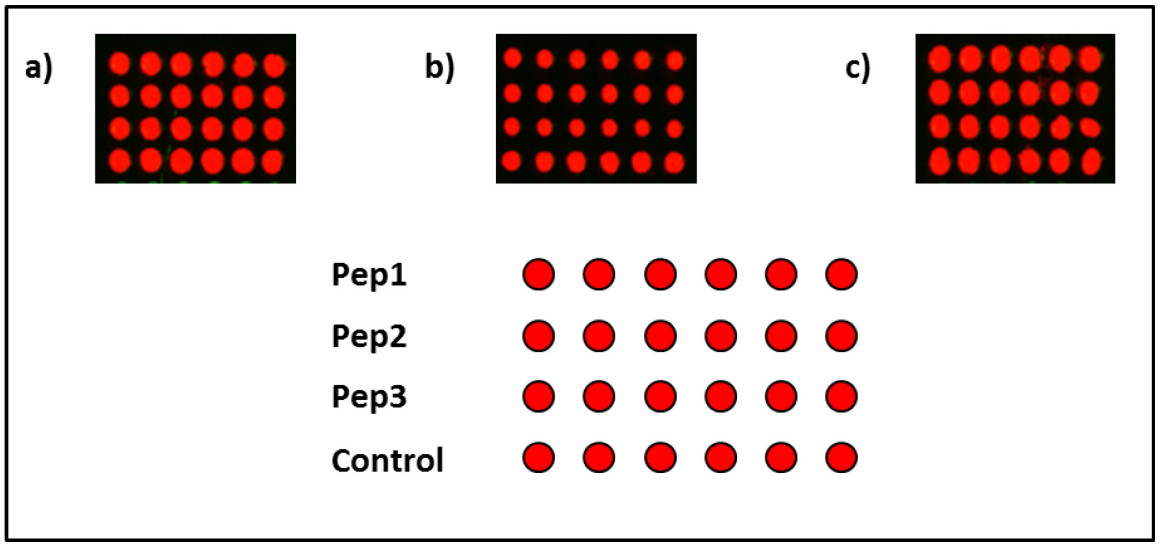

Figure 32: Test staining after peptide spotting (5 replicates); a) dextran coating, b) PEGMA/MMA coating, c) dextran coating after chemical stress test. Streptavidin staining was performed using a 1:5000 dilution out of a 10mg/ml stock solution; Read out was performed on the Odyssey scanner for near-infrared dyes (intensity 4).

Figure 32 shows the spotted peptide pattern on dextran and PEGMA/MMA polymer after streptavidin staining. Compared to PEGMA, the spots on dextran show a slightly extended spot morphology which indicates an increased wettability of the coating. The chemical stress test of the new dextran films with TFA and piperidine showed no negative influence. As depicted in Figures 33 and 34, proteolysis on dextran surfaces show a similar decrease in fluorescence intensity with trypsin compared to the standard PEGMA films. With thrombin

however an optimization of around 20% could be achieved. As next step a kinetic measurement was performed to check for sensitivity, especially for shorter time points. Figure 35 shows the trypsin incubation over two hours with four time points measured.

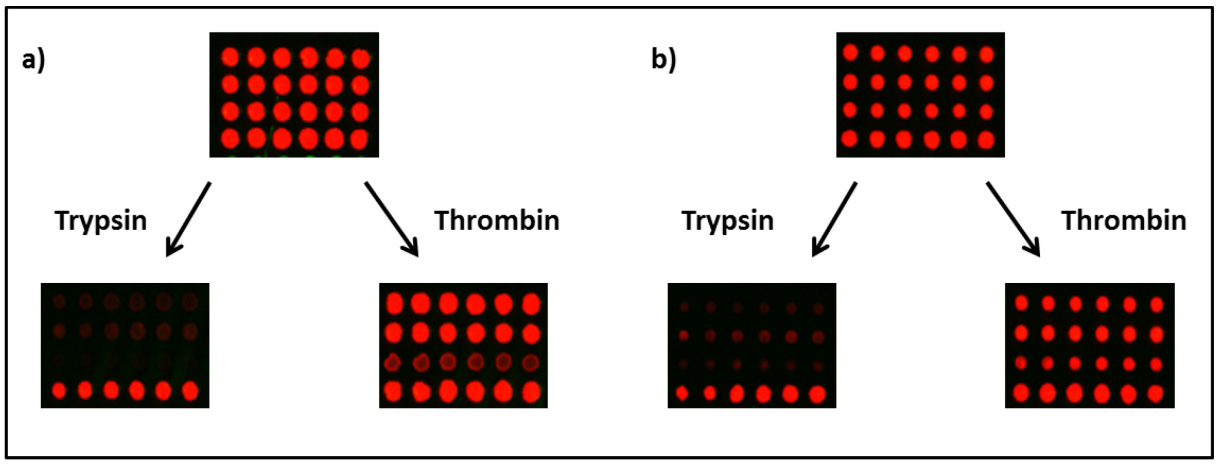

Figure 33: Enzyme digestion of spotted peptide pattern; a) dextran coating, b) PEGMA/MMA coating. Enzyme incubation was carried out 2h at 37°C; streptavidin staining was performed using a 1:5000 dilution out of a 10mg/ml stock solution; Read out was performed on the Odyssey scanner for near-infrared dyes (intensity 4).

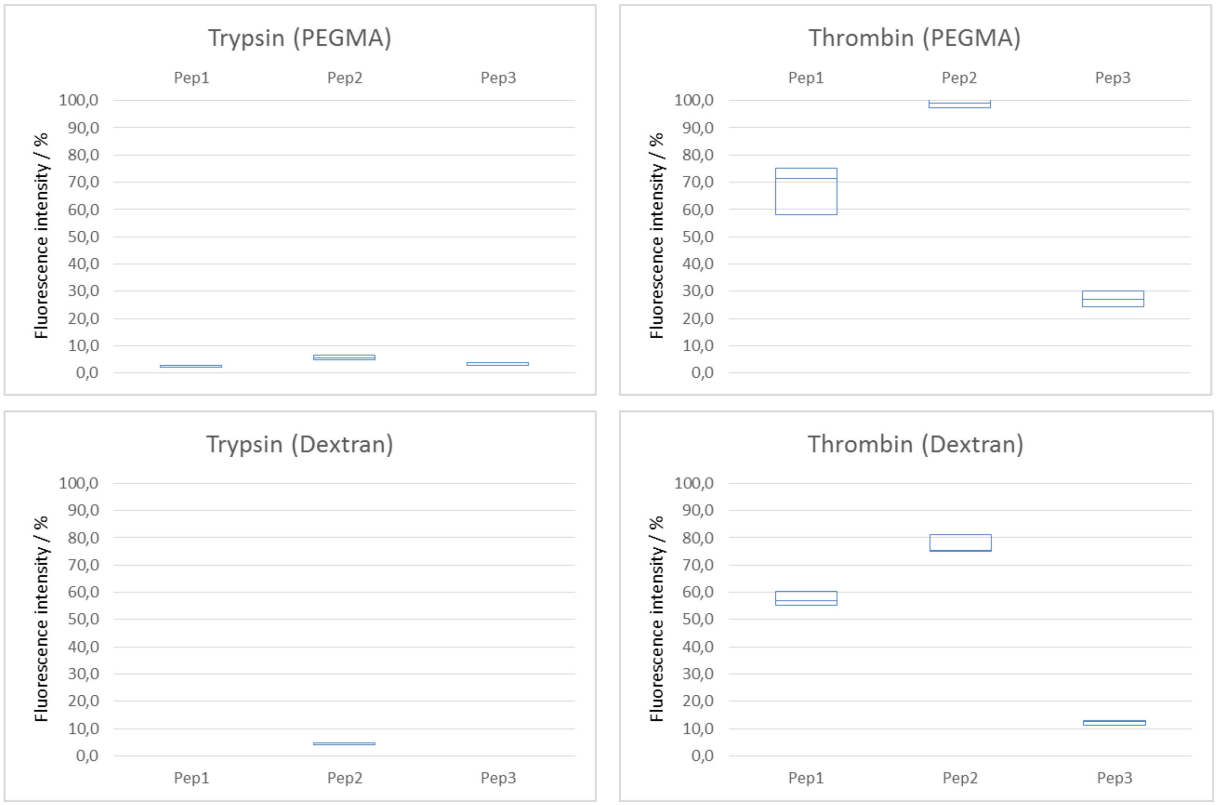

Figure 34: Quantification data of spotted peptide array after 5µM enzyme incubation at 37°C for 2h (fluorescence scan not shown). For analysis the average over identical replicates was taken; Analysis was performed using the PepSlideAnalyzer Software.

Proteolysis with thrombin on the other hand showed an overall increase in digestion of about 20% for peptide 1 and 3, as depicted in Figure 36. Peptide 2 though, having the cleavage site C-terminally located, is hardly cleaved by thrombin on both coatings. It has to be taken into account that this model system is not representative for every enzyme but at least the dextran polymer turned out to be a promising alternative to the PEGMA film. Its synthesis process is cheap and does not need excessive volumes of organic solvents compared to the PEGMA-based polymers. Further the production can easily be up-scaled. As a next step a standard 22 x 21 cm glass plate was coated with dextran and introduced into the in-situ peptide synthesis at PEPperPRINT© GmbH.

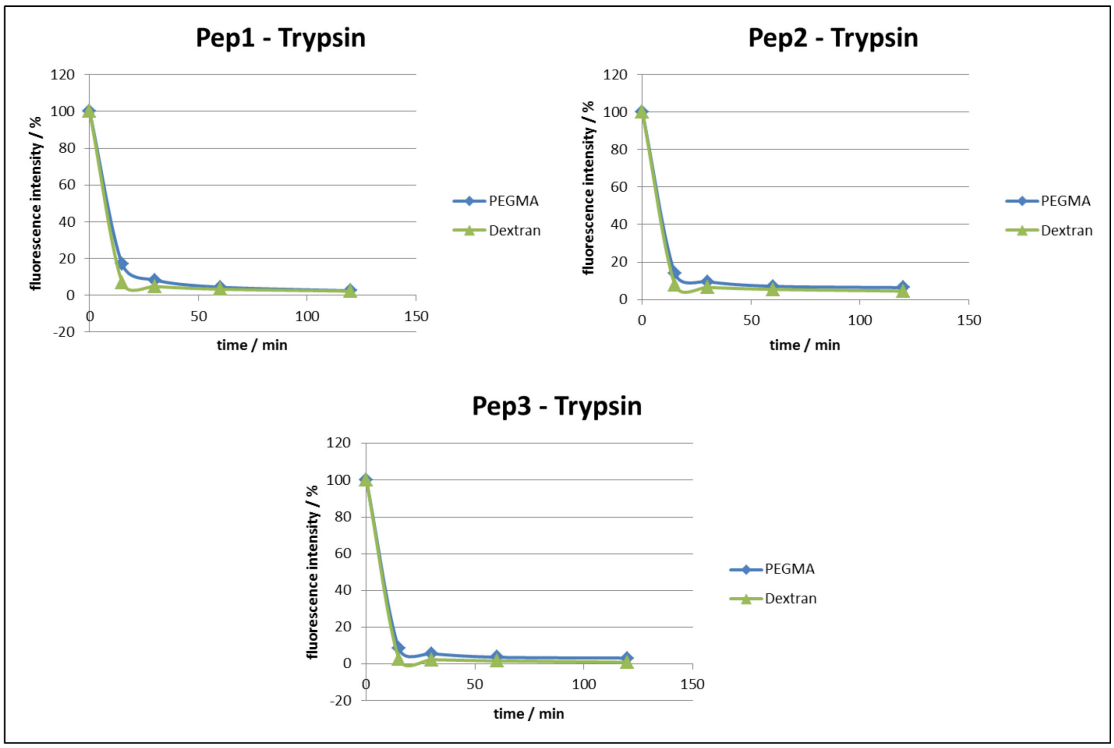

Figure 35: Kinetic measurement of spotted sample peptides using 5µM trypsin as digesting enzyme over 2h at 37°C on dextran and PEGMA surfaces.

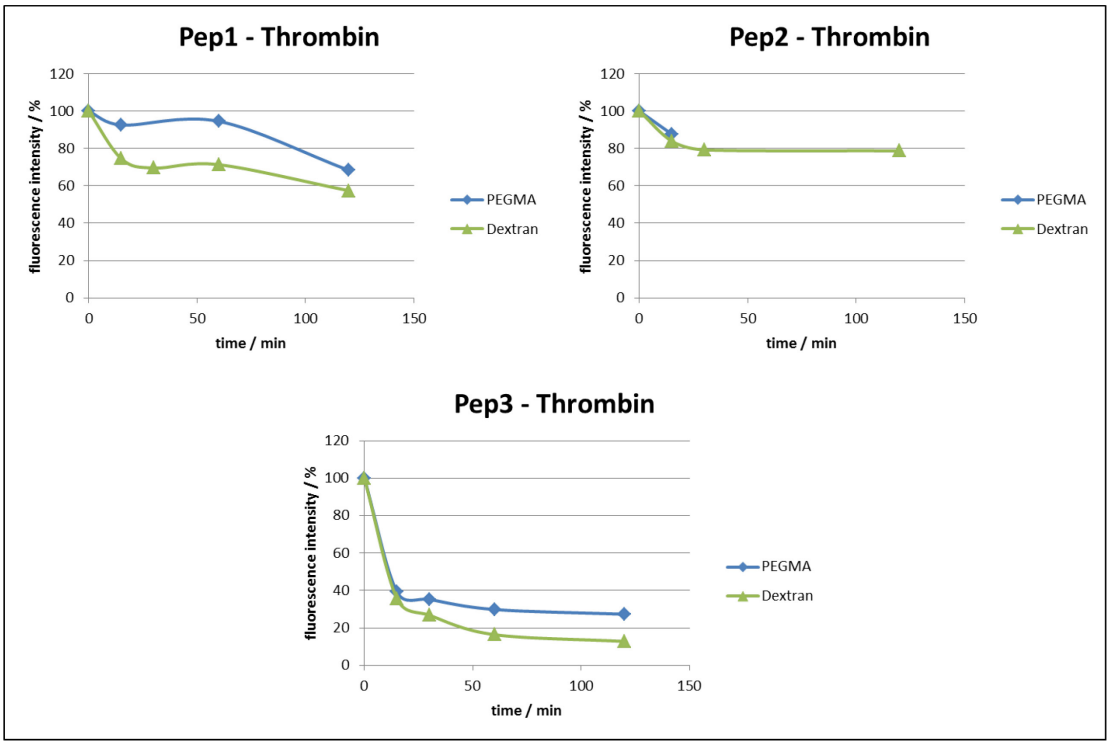

Figure 36: Kinetic measurement of spotted sample peptides using 5µM thrombin as digesting enzyme over 2h at 37°C on dextran and PEGMA surfaces.

III.2.1.3. Dextran coating in the in-situ synthesis

For testing the new dextran polymer in the in-situ synthesis, the surface coating was performed using the optimized conditions discussed in the last chapter (2.5% APTES solution & 2.5% CM-Dextran solution). Prior to the actual SPPS, a standard linker (2 β-alanine + aspartic acid) was printed to set up the synthesis pattern. After the peptide synthesis a comparison of the peptide load, quantified via OD-measurement after Fmoc-cleavage, showed an average peptide load of ~1.46nmol/cm^2 for dextran; compared to the standard PEGMA/MMA films with about ~0.84nmol/cm^2, this about 1.7 fold higher value however could be a disadvantage for a protease assay because of the higher amount of peptides that have to be digested. This would lead to an increased amount of time or higher enzyme concentration needed, compared to the PEGMA/MMA surface. The test staining showed a similar spot morphology like using standard PEGMA/MMA-polymers. Figure 37 shows exemplary an enzymatic digestion with the model proteases proteinase k and trypsin. For both proteases an overall decrease in fluorescence intensity of around 30% was yielded. In order to compensate the higher peptide load, higher enzyme concentrations as well as a longer incubation time were checked. Unfortunately even with a 10 fold higher enzyme

concentration and an incubation time of 18 hours, no significantly increase in proteolytic digestion could be achieved.

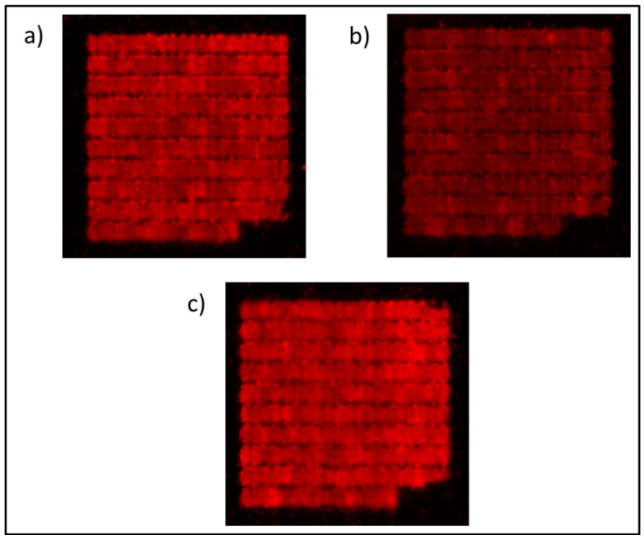

Figure 37: Peptide content with N-terminal printed biotin [in-situ synthesis on dextran film]; a) 5µM trypsin, b) 5µM proteinase K; c) Buffer control. Enzyme incubation was carried out for 2h at 37°C; streptavidin staining was performed using a 1:5000 dilution out of a 10mg/ml stock solution; Read out was performed on the Odyssey scanner for near-infrared dyes (intensity 4).

In summary it could be shown that polysaccharide-based polymers like dextran are a good alternative surface coating compared to the standard PEGMA/MMA films used so far in terms of easy applicable synthesis process, upscaling to production parameters and low costs. Preliminary experiments using standard microscopy glass slides and pre-synthesized spotted peptides showed promising results using model proteases. In the next step this new dextran synthesis method was transferred to the production scale at *PEPperPRINT© GmbH.* The first batch of in-situ PEPperChips™ showed an almost 2 fold higher peptide load compared to the standard PEGMA/MMA coatings but comparable spot morphologies and sufficient fluorescence intensity in the tests, both with antibody and streptavidin staining. However preliminary protease experiments showed an insufficient digestion of the peptides on the new implemented surface coating, even with 10 fold higher enzyme concentrations and elongated incubation times. It has to be taken into account that optimization of the dextran polymer is ongoing and the whole surface and peptide synthesis process takes around 5 to 6 weeks per batch. Further the transfer of lab to production scale is not fully comparable because of the use of pre-synthesized, spotted peptides against the in-situ synthesis. Using micro-particle based peptide synthesis (mpSPPS), the surface polymer is stressed with chemicals resulting from the coupling procedures, the matrix of the micro-particles, etc. in every synthesis cycle (~35 to 50 cycles, dependent on the peptide length) whereas in lab scale only one mild coupling step is performed.

IV. Conclusion

Conclusion

The aim of the present work was to develop an enzymatic assay system based on combinatorically synthesized peptide microarrays, manufactured in close cooperation with the company *PEPperPRINT© GmbH*. This goal was achieved by introducing a specific label N-terminally to the peptide sequences which can be stained and read out after protease incubation via fluorescence measurement. To check for general applicability the peptide arrays were synthesized with N-terminal located antibody tags (*FLAG* & *HA*), by using the standard micro-particle based peptide synthesis (mpSPPS) without further chemical modification. After protease incubation only fully intact, tagged peptide sequences are stained with their specific, fluorescently labeled antibodies. The decrease in fluorescence intensity represents the enzymatic activity. The results using trypsin and proteinase k as model enzymes were promising. To address a broader range of proteases, biotin as non-proteinogenic label was introduced, after being available as micro-particle based building block, which cannot be falsely cleaved, like an antibody tag, but specifically stained by using a fluorescently labeled streptavidin. It turned out to be advantageous to stick to the mpSPPS method for labeling the peptide content with biotin, to reduce nonspecific binding to the polymer surface, like found when performing in-solution labeling experiments. A direct labeling via fluorescent dyes to yield an on-demand measurement approach however was not successful; due to the high contamination risk and technical difficulties, fluorescent dyes could not be embedded into micro-particles for the in-situ synthesis. With the established biotin-streptavidin system and the corresponding model proteases, kinetic data varying enzyme concentration as well as incubation time, was obtained. In order to optimize the on-chip proteolysis, an alternative surface coating based on polysaccharides was prepared. The experimental dextran polymer showed promising results in lab scale, using spotted peptides. Further the easy synthesis process and up-scaling to production parameters, together with the low costs compared to the standard PEGMA/MMA coating, are a major advantage. After transferring the new coating procedure to production scale, the resulting peptide load turned out to be around 1.7 fold higher than on PEGMA/MMA which seems in consequence to be too high for a proper enzymatic digestion on a solid support. Here a decrease in fluorescence intensity down to 70% using proteinase k could be obtained which indicates the need of optimization.

Outlook

In principle enzymatic activity in a sample of interest can be measured with peptide microarrays. The established model system has shown that the protease assay can be directly performed on the biotin labeled *PEPperCHIP™* arrays without modification.

To further optimize the assay system several tasks remain. First of all the surface polymer has to be modified in a way that a preferably high number of proteases can be addressed in terms of accessibility of their cleavage sites. Preliminary experiments with the alternative dextran coating yielded a high peptide load, compared to the standard PEGMA/MMA, which is not feasible for the targeted assay system. A reduction here should lead to higher cleavage efficiencies, plus less need of incubation time and enzyme concentration in the sample; together with an optimization of the polymer synthesis, regarding the silanization and dextran modification steps, to obtain an optimum film thickness, this will lead probably to a more sensitive monitoring. In the present work silanization and the following adding of dextran, corresponding to an approximate film thickness of ~100nm after silane and ~15nm for the final film, showed promising results in lab scale using spotted peptides. The transfer to production scale at *PEPperPRINT© GmbH* is still an ongoing process and will be pursued in the future. Furthermore the overall applicability of the dextran polymer for all experimental approaches offered on standard PEGMA/MMA based *PEPperCHIP´s™* has to be further studied.

Another task in the future will be to further investigate the possibility of a direct labeling approach using fluorescent dyes or other on-demand measurement techniques. In the present work the difficulties of specifically labeling in-situ synthesized peptides out from solution have been discussed. If it would be possible in the future to embed fluorescent dyes into the mpSPPS production process, this would be a major advantage.

Although there are still some parameter to be further investigated, the established model system already shows the general applicability of high density peptide microarrays as tool for measuring protease activity. With further optimization, this work paves the way for testing clinical samples so that such arrays can help to advance the field of peptide marker screenings in the future.

V. Material & Methods

V.1. Devices & Measuring parameters

V.1.1. Ellipsometry

Film thicknesses were measured with an M-44 multiple wavelength ellipsometer (*J. A. Woollam Co. Inc.,* Lincoln, NE/USA). Sample alignment was at a nominal incidence angle of 75° to the surface normal. Polymer layer thicknesses were determined using the appendant *WVASE* software and a single *CAUCHY* model layer[81]. Clean Si(100) wafers kept in air are usually covered with a 21-25 Å thin SiO_2 layer[82,83] on which SAMs of organo-silanes can be assembled as an anchor group for polymers. The thickness of the polymer coating in such multilayered systems was determined by measuring the sample against a UV- or acid-cleaned reference wafer (silicon bulk + silicon oxide). Assuming homogeneous molecular packing (silicon bulk + silicon oxide + organic layer) the CAUCHY model was used to fit the thickness of the organic layers.

V.1.2. Fluorescence Scans

Fluorescence scans were performed with the *Odyssey Infrared Imager* (*LI-COR Biosciences*, Lincoln, NE/USA) or the *GenePix 4000B Microarray Scanner* (*Molecular Devices*, Sunnyvale, CA/USA) depending on the wavelength of the used fluorescent dye.

Odyssey Infrared Imager

The *Odyssey Infrared Imager* is equipped with two solid state lasers simultaneously providing light excitation at 685 and 785 nm. Accordingly the Odyssey was used to scan samples stained with the *DyLight680* and *DyLight800* dyes. Image acquisition was performed with the *Odyssey Application Software 3.0 (V. 3.0.21)*. The *Odyssey Infrared Imager* was routinely set to 21 µm resolution and a detector intensity of 4.0 for streptavidin-DL680 stained samples and 7.0 for Anti-*HA*-DL680 stained samples. Quantitative analyses were performed with the *SICASYS PepSlide Analyzer Software* (*V. 2.0.9.*).

GenePix 4000B Microarray Scanner

The *GenePix 4000B Microarray Scanner* is a microscopy slide scanner equipped with two solid state lasers providing simultaneous light excitation at 532 and 635 nm. Accordingly the *GenePix* was used to scan samples stained with *TAMRA, DyLight550* and *Benzofurazan* dyes. Image acquisition was performed with the *GenePix Pro 6.0 Acquisition and Analysis Software*. The scan resolution was set to 5 µm, scan power to 33 % and PMT (photo multiplier tube) between 300 and 500, depending on fluorescence intensity in a pre-scan. PMT values above 500 lead to interferences due to auto-fluorescence of the glass and should be avoided.

V.1.3. Spotting Robot

The peptide arrays were spotted using the *BioRobotics Microgrid II* spotting *robot* with a single contact spotting tip. Each peptide solution was prepared in filtered PBS-T (pH 7.4, 0.15 M) and filled in *Small Volume 384 Well Plates* (*Greiner Bio-One GmbH*, Frickenhausen/Germany). Spotting layout and gal-file export were performed with the *TAS Application Suite* (*V. 2.4.0.3*).

V.2. Materials

V.2.1. Chemicals & Solvents

DyLight680-streptavidin (*Pierce Protein Research Products*), DyLight550-Phosphine and SMCC were obtained from *Thermo Fisher Scientific* (Geel/Belgium).

Biotin-OPfp was purchased from *Iris Biotech GmbH* (*Marktredwitz/Germany*).

TFA (≥99.9 %), Ac_2O (≥99 %), DIPEA (≥99 %), DCM (≥99.9 %), KH_2PO_4 (≥99 %), $Na_2HPO_4 \cdot 2\ H_2O$ (≥98 %) and DMSO (≥99.5 %) were obtained from *Carl Roth* (*Karlsruhe/Germany*).

TRIS (≥99.9 %) was obtained from *Santa Cruz Biotechnology Inc.* (*Dallas, TX/USA*).

DMF (≥99.8 %) and HCl (37 %) were purchased from *VWR International* (*Radnor, PA/USA*). ACN (HPLC-grade) was obtained from *VWR International S.A.S.* (*Fontenay-sous-Bois/France*).

KOH (p.a.) and DCM (≥98.9 %, anhydrous) were purchased from *AppliChem GmbH* (*Darmstadt/Germany*).

PVP (M_W= 40,000 g/mol) and KCl (99.5 %) were obtained from *Merck KGaA* (*Darmstadt/Germany*). HBTU was obtained from *Merck Schuchardt OHG* (*Hohenbrunn/Germany*).

HOBt (anhydrous) was obtained from *Molekula Ltd.* (*Dorset/UK*).

All used PEG-derivatives were obtained from *Rapp Polymere GmbH* (*Tübingen/Germany*).

TAMRA-5-Maleimide (≥95 %), TAMRA-5-NHS, TAMRA-5-COOH (≥95 %), Fmoc-β-azido-Ala-OH (≥98 %), Tween20, EtOH (p.a.), MeOH (p.a.), ^{i}PrOH (p.a.), acetone (p.a.), β-mercaptoethanol (min. 98%), NaCl (≥99 %), 4-chloro-7-nitro-benzofurazan, DMF (anhydrous, 99.8 %), CDI, APTES (≥98 %), piperidine (99 %), Trizma® base (≥99.9 %), $CaCl_2 \cdot 2\ H_2O$ (≥99.9 %), CM-Dextran sodium salt, NHS (98 %) and NH_2-Maleimide-Linker (≥95 %) were obtained from *Sigma-Aldrich GmbH* (*Steinheim/Germany*). All chemicals and solvents were used without further purification.

Syringe filters were purchased from *Sartorius Stedim Biotech GmbH* (*Göttingen/Germany*).

Nitrogen (5.0, P200) was purchased from *Guttroff GmbH* (*Wertheim-Reichholzheim/Germany*). For washing steps and buffers solely *Milli-Q-filtered* water (*Millipore Corporation, Merck KGaA*, *Darmstadt/Germany*, resistivity ~ 18.2 MΩcm) was used.

V.2.2. Pre-synthesized peptides

All pre-synthesized peptides were purchased from *Peps4LifeSciences GmbH* (*Heidelberg/Germany*) and used as delivered.

V.2.3. Buffers, Antibodies, Enzymes

PBS-T

0.15 M phosphate buffer saline (PBS) containing additional 0.05 % (v/v) Tween20 (PBS-T) was freshly prepared before use. 8.00 g NaCl (137.00 mmol), 0.20 g KCl (2.7 mmol), 1.44 g $Na_2HPO_4 \cdot 2\ H_2O$ (8.1 mmol) and 0.20 g KH_2PO_4 (1.5 mmol) were solved in water. The

solution was adjusted to pH 7.4 with HCl and filled up to 1 L. After filtration 500 µl Tween20 were added under constant stirring.

TBS-T

0.20 M TRIS-buffer saline (TBS) containing additional 0.05 % (v/v) Tween20 (TBS-T) and 25 mM Calcium was freshly prepared before use. 6.00 g Trizma® base (50 mmol), 8.80 g NaCl (150 mmol) and 11.60 g $CaCl_2 \cdot 2\ H_2O$ (20 mmol) were solved in water. The solution was adjusted to pH 7.4 with HCl and filled up to 1 L. Afterwards 500 µl Tween20 were added under constant stirring.

Rockland buffer

Rockland Blocking Buffer for Fluorescent Western-Blotting (Rockland buffer) was obtained from *Rockland Immunochemicals Inc.* (*Gilbertsville, PA/USA*) and used as received.

Antibodies

The monoclonal mouse-anti-*HA* 12CA5 IgG antibody (Anti-*HA*) was obtained from Dr. Gerhard *Moldenhauer* (*German Cancer Research Centre (DKFZ), Heidelberg/Germany*). The monoclonal mouse-anti-*FLAG* M2 IgG antibody (anti-*FLAG*) was purchased from *Sigma-Aldrich GmbH* (*Steinheim/Germany*). The monoclonal anti-MEY-ac OVA antibody (anti-acetyl-lysine antibody) was obtained from *David Biotech* (*Technical University Darmstadt (TUDa), Darmstadt/Germany*). The goat anti-rabbit IgG (H+L) antibody (Dylight™680 conjugated) was obtained from *Thermo Scientific* (Germany). Fluorescent labels were attached by Jürgen *Kretschmer* (*German Cancer Research Centre (DKFZ), Heidelberg/Germany*) using commercial labeling kits and the respective protocols which were recommended by the manufacturers. Labelling kits for DyLight680 and DyLight800 were obtained from *Innova Biosciences Ltd.* (*Cambridge/UK*).

Enzymes

All purchased enzymes were portioned in 50 µl aliquots and stored under -20°C. Trypsin (from porcine pancreas, 1 mg tablet, dissolved following the manufacturers protocol), thrombin (from bovine plasma, 40-300 NIH), elastase (from porcine pancreas, ≥4 NIH) and

chymotrypsin (Type VII, TLCK treated, ≥40 NIH) were obtained from *Sigma-Aldrich GmbH* (*Steinheim/Germany*). Proteinase k (20 mg/ml solution) was purchased from *Genaxxon Bioscience GmbH* (*Ulm/Germany*).

V.2.4. Microarray surfaces

For all self-manufactured surfaces in lab scale, standard microscopy glass slides from *Marienfeld* (*Lauda-Königshofen/Germany*) were used.

V.2.5. Peptide microarrays

All peptide microarrays were purchased from *PEPperPRINT GmbH* (*Heidelberg/Germany*). Upscaling of the dextran surface coating (see V.3. Methods) and testing was performed together with *PEPperPRINT GmbH*.

V.3. Methods

V.3.1. Preparation of synthesis surfaces

In the present work standard microscopy glass slides were equipped with a synthesis coating. The derivatization of Si(100) wafers was routinely performed in petri dishes (V≈50 ml). Microscopy glass slides were treated in batches of 5 to 10 slides in standard glass washing chambers (V≈ 200 ml) and petri dishes (V≈ 100-200 ml). The 22 x 21 cm^2 glass slides used in large scale at *PEPperPRINT GmbH* were coated in a custom-built Teflon incubation container (V≈ 1 L).

V.3.1.1. Cleaning & Activation

Glass surfaces were cleaned and activated by overnight treatment with 1M KOH in 2-propanol. The surfaces were intensively washed with water, rinsed with acetone and dried in

a stream of air. After heating to 100°C for 1h the slides were allowed to cool to RT and stored under -20°C and inert gas atmosphere till use.

Si(100) wafers were activated by UV radiation for 1h in air at *PEPperPRINT GmbH*. UV radiation was generated with a 150 W mercury vapor lamp (*Heraeus Noblelight GmbH, Hanau/Germany*, model TQ150, purchased from *UV consulting Peschl, Mainz/Germany*). The surface was put in about 4 cm distance from the lamp. After cooling to RT the wafers were directly used for further silanization.

For lab scale the wafers were activated by overnight incubation in caro acid (50% H_2SO_4 in H_2O_2). The surfaces were intensively washed with water and dried at 100°C before further use.

V.3.1.2. Self-assembly of APTES

A solution of 2.5% APTES (v/v) in anhydrous DCM was prepared and directly added to the dry, activated surfaces. The surfaces were left to react overnight. Subsequently, the DCM was stepwise replaced with ethanol. The surfaces were washed three times 5 min each with ethanol, two times 5 min each with acetone, dried in a stream of air and baked in a pre-heated oven at 100°C for 2h. After cooling to RT the slides were either used directly for dextran coating or stored at -20°C under nitrogen. In some cases rests of precipitated colorless powder had to be removed by 15 min ultra-sonication in ethanol.

V.3.1.3. Dextran coating

Dextran films were grafted on the silanized surfaces according to the following protocol: 2.5 g CM-Dextran (≈ 50 mg/ml), 1.62 g CDI (10 mmol) and 1.15 g NHS (10 mmol) were mixed in 50 ml Milli-Q-water. The pH value was adjusted to pH 8.0 with NaOH and then filtered with a standard syringe filter (5.00 µm). The filtered solution was then added to the surfaces in a petri dish and left to react overnight under constant shaking at RT. Subsequently, the surfaces were washed three times 5 min each with Milli-Q-water and two times 5 min each with DMF. After rinsing with acetone, the surfaces were blown dry in a stream of air and stored under -20°C and nitrogen till further use.

For coating of production scale plates at *PEPperPRINT© GmbH* the reaction was up-scaled to the required volume. A piece of silanized Si(100) was added to the reaction as a reference to determine the respective film thickness via ellipsometry.

V.3.1.4. Capping of dextran coatings

Dextran surfaces were capped according to following protocol: A freshly prepared solution of 10 % ESA, 20 % DIPEA and 70 % DMF (v/v) was added to the slides three times 30 min each. Subsequently, the surfaces were washed three times 5 min each with DMF, two times 5 min each with MeOH and 5 min with acetone. After rinsing with acetone the slides were blown dry in a stream of air and stored under -20°C and nitrogen till further use.

V.3.1.5. Amino-functionalization of dextran

Dextran coatings were amino-functionalized according to following protocol: 2.43 g CDI (15 mmol) was mixed with 50 ml ACN and the solution added to the surfaces. The slides were left to react 30 min at RT under constant shaking and then washed once 5 min with ACN. 1.26 ml 1,3-diaminopropane (15 mmol, 1.11 g) was mixed with 50 ml ACN and the solution added to the surfaces. The slides were left to react 1h at RT under constant shaking. Subsequently, the surfaces were washed three time 5 min each with ACN and two times 5 min each with MeOH. After rinsing with acetone the slides were blown dry in a stream of air and stored under -20°C and nitrogen till further use.

V.3.2. Coupling of SMCC, NH_2-Mal-Linker & Spotting

A solution of 3 mM SMCC in anhydrous DMF was prepared. Amino-functionalized surfaces were placed in a petri dish and covered with 1 ml of the SMCC solution each. After 2h incubation the slides were washed three times 5 min each with DMF, two times 5 min each with MeOH and 5 min with acetone. After rinsing with acetone the surfaces were dried in a stream of air and either used directly for further spotting experiments or stored under -20°C and nitrogen till further use.

After peptide spotting the slides were left to react for additional 90 min and then rocked for 60 min in a solution of 5 % β-mercaptoethanol in EtOH (v/v). The slides were then washed three times 5 min each with EtOH and 5 min with acetone and afterwards dried in a stream of air.

V.3.3. Micro particle-based peptide synthesis

Micro particles containing Opfp-activated and Fmoc-protected amino acids or Opfp-activated biotin were selectively addressed onto the linker-modified surfaces using the laser printer technique[49]. The peptide synthesis on the 22 x 21 cm^2 glass slides was commissioned to the *PEPperPRINT GmbH* (*Heidelberg/Germany*).

V.3.4. N-terminal modification of printed Peptides from Solution

V.3.4.1. Biotin-Opfp

To couple Biotin-Opfp to the N-termini of printed peptides, a solution of 2.4 mM Biotin-Opfp in anhydrous DMF was prepared. The surfaces were placed in a petri dish and covered with 1 ml of the coupling solution and left to react overnight at RT. The slides were washed three times 5 min each with DMF, two times 5 min each with MeOH and 5 min with acetone. After rinsing with acetone the slides were blown dry in a stream of air and stored under -20°C and nitrogen till further use.

V.3.4.2. TAMRA-COOH, Fmoc-TAMRA-Lys-OH & Fmoc-β-N_3-Ala-OH

To couple TAMRA-COOH, Fmoc-TAMRA-Lys-OH & Fmoc-β-N_3-Ala-OH to the N-termini of printed peptides, a solution of 1 mM TAMRA-COOH, 10 mM Fmoc-TAMRA-Lys-O or 10 mM Fmoc-β-N_3-Ala-OH in anhydrous DMF was prepared. The same volume of a solution of 10 mM HOBt, 10 mM HBTU and 10 mM DIPEA was added. The surfaces were placed in a petri dish and covered with 1 ml of the coupling solution and left to react overnight at RT. The slides were washed three times 5 min each with DMF, two times 5 min each with MeOH and 5 min with acetone. After rinsing with acetone the slides were blown dry in a stream of air and stored under -20°C and nitrogen till further use.

V.3.4.3. TAMRA-NHS

To couple TAMRA-NHS to the N-termini of printed peptides, a solution of 20µM TAMRA-NHS in PBS-T was prepared. The surfaces were placed in a petri dish and covered with 1 ml of the labeling solution and left to react for 2h at RT. The slides were washed three times 5 min each with PBS-T, two times 5 min each with Milli-Q-water, blown dry in a stream of air and stored under -20°C in an inert gas atmosphere till further use.

V.3.4.4. Atto680-Mal, Dylight800-Mal & TAMRA-Mal

To couple Atto680-Mal, Dylight800-Mal & TAMRA-Mal, a solution of 0.3µM Atto680-Mal 0.3µM Dylight800-Mal or 0.7µM TAMRA-Mal in PBS-T was prepared. The surfaces were placed in a petri dish and covered with 1 ml of the labeling solution and left to react for 2h at RT. The slides were washed three times 5 min each with PBS-T, two times 5 min each with Milli-Q-water, blown dry in a stream of air and stored under -20°C in an inert gas atmosphere till further use.

V.3.4.5. FlAsH-EDT$_2$

To couple FlAsH-EDT$_2$, a solution of 7.5mM FlAsH-EDT$_2$ in PBS-T with 0.1M DTT was prepared. The surfaces were placed in a petri dish and covered with 1 ml of the labeling solution and left to react for 2h at RT. The slides were washed three times 5 min each with PBS-T, two times 5 min each with Milli-Q-water, blown dry in a stream of air and stored under -20°C in an inert gas atmosphere till further use.

V.3.4.6. Dylight550-Phosphine & TAMRA-PEG(3)-N$_3$

To couple Dylight550-Phosphine & TAMRA-PEG(3)-N$_3$, a solution of 10µM Dylight550-Phosphine & TAMRA-PEG(3)-N$_3$ in PBS-T was prepared. The surfaces were placed in a petri dish and covered with 1 ml of the labeling solution and left to react for 4h at 37°C. The slides were washed three times 5 min each with PBS-T, two times 5 min each with Milli-Q-

water, blown dry in a stream of air and stored under -20°C in an inert gas atmosphere till further use.

V.3.5. Blocking

V.3.5.1. PVP-Blocking prior to enzyme incubation

To block the surfaces prior to enzyme incubation, a solution of 2% (m/v) PVP (M_W=40000) in TBS-T was prepared. The surfaces were placed in a 16 well incubation chamber, the target wells covered with 200µl of the blocking solution and left to react for 1h at RT.

V.3.5.2. Rockland-blocking

To block the surfaces prior to antibody or streptavidin staining, *Rockland buffer* was used directly without dilution. The surfaces were placed in a 16 well incubation chamber, the target wells covered with 200µl of the blocking solution and left to react for 1h at RT.

V.3.6. Enzyme incubation

For protease incubation, a solution of 5µM of the target enzyme in 0.2% (m/v) PVP (M_W=40000) TBS-T was prepared. The surfaces were placed in a 16 well incubation chamber, the target wells covered with 200µl of the protease solution and left to react for 2h at 37°C. The slides were washed three times 5 min each with TBS-T and used further for staining.

V.3.7. Antibody staining

V.3.7.1. Anti-FLAG/anti-HA antibodies

For staining of the *FLAG/HA* antibody tags, a dilution of 1:1000 out of a stock solution (anti-*HA*: 95µg/ml in PBS + 0.02% NaN_3 + 10% Rockland buffer; anti-*FLAG*: 0.21mg/ml in PBS + 0.02% NaN_3 + 10% Rockland buffer) of a monoclonal mouse-anti-*HA* 12CA5 IgG antibody

(Anti-*HA*) or monoclonal mouse-anti-*FLAG* M2 IgG antibody (anti-*FLAG*) respectively in TBS-T with 10% (v/v) *Rockland buffer* was prepared. The surfaces were placed in a 16 well incubation chamber, the target wells covered with 200µl of the staining solution and left to react for 1h at RT. The slides were washed three times 5 min each with PBS-T, two times 5 min each with Milli-Q-water, blown dry in a stream of air and stored under 4°C in an inert gas atmosphere.

V.3.7.2. Anti-Ac-Lys-staining

For staining of the acetylated lysine residues, a dilution of 1:20000 out of a stock solution (primary: 2.08mg/ml in PBS + 0.02% NaN_3; secondary: 1mg/ml in PBS + 1% BSA + 0.02% NaN_3) of a monoclonal anti-MEY-ac OVA antibody (anti-acetyl-lysine antibody, primary) and a dilution of 1:5000 of a goat anti-rabbit IgG (H+L) antibody (Dylight^{TM}680 conjugated, secondary) in 0.2% PVP (m/v) TBS-T respectively was prepared. Prior to antibody staining the surfaces were blocked with 2% (m/v) PVP (see V.3.5.1.). The surfaces were placed in a 16 well incubation chamber, the target wells covered with 200µl of the staining solution and left to react for 30min for the primary and 1h for the secondary antibody at RT. The slides were washed three times 5 min each with PBS-T, two times 5 min each with Milli-Q-water, blown dry in a stream of air and stored under 4°C in an inert gas atmosphere.

V.3.8. Streptavidin staining

For staining of biotinylated surfaces, a dilution of 1:5000 out of a stock solution (1mg/ml in PBS + 0.02% NaN_3) of Dylight^{TM}680 conjugated streptavidin in TBS-T with 10% (v/v) *Rockland buffer* was prepared. The surfaces were placed in a 16 well incubation chamber, the target wells covered with 200µl of the staining solution and left to react for 1h at RT. The slides were washed three times 5 min each with PBS-T, two times 5 min each with Milli-Q-water, blown dry in a stream of air and stored under 4°C in an inert gas atmosphere.

V.3.9. Spotting of pre-synthesized peptides using the BioRobotics Microgrid II spotting robot

For all spotting experiments pre-synthesized peptides purchased from *Peps4LifeSciences GmbH* were used as delivered and diluted in Milli-Q-water to yield a 1mM stock solution,

stored at -20°C till further use. For spotting a final concentration of 50µM diluted in PBS-T was used. After spotting the slides were left to react for another 90min at RT, blocked with a 10% (v/v) mercaptoethanol in ethanol solution for 1h at RT and washed three times 5 min each with ethanol, two times 5 min each with acetone and blown dry in a stream of air and stored under -20°C in an inert gas atmosphere till further use.

V.3.10. Micro-particle based peptide synthesis

Micro particles containing the Opfp-activated Biotin or Opfp-activated and Fmoc-protected amino acids were selectively addressed onto the dextran modified surfaces using the laser printer technique.[49] The peptide synthesis on the 22 x 21cm^2 glass plates was commissioned to the company *PEPperPRINT© GmbH (Heidelberg/Germany)*. Then the solid supports were transferred into a pre-heated oven and allowed to react at 90°C for 90 min under nitrogen atmosphere. After cooling to RT, unreacted amino groups were capped with 10% (v/v) Ac_2O, 20% (v/v) DIPEA and 70% (v/v) DMF; Glass slides/plates were rocked in an excess of this mixture for 30 min. Subsequently, the surfaces were washed three times 5 min each with DMF and 5 min with acetone. The surfaces were either stored at 4°C under argon atmosphere or directly deprotected for the next coupling cycle. To cleave the Fmoc protecting group, the glass slides/plates were rocked in a solution of 50% (v/v) piperidine in DMF for 30 min. Subsequently the surfaces were washed three times 5 min each with DMF, two times 5 min each with MeOH and 5 min with acetone and then blown dry in a stream of compressed air. Then the next particle deposition was performed.

V.4. Analytical techniques

V.4.1. UV/Vis Photospectrometry

In standard SPPS following the Fmoc-protection strategy, before each coupling cycle the N-terminal Fmoc-protecting group has to be cleaved prior to attachment of the next building block. The piperidine dibenzofulvene adduct (PDFA) resulting from the reaction as intermediate product has an absorption maximum at 301nm (Figure 38). The concentration of the PDFA adduct in the deblocking solution can be measured using UV/Vis Photospectrometry comparing its absorption with a blanc solution. Based on that, the amino

group loading and therefore the peptide load in nmol/cm^2 on the surface can be calculated following the *Lambert-Beer´s* law (see equation 1).[84,85,86]

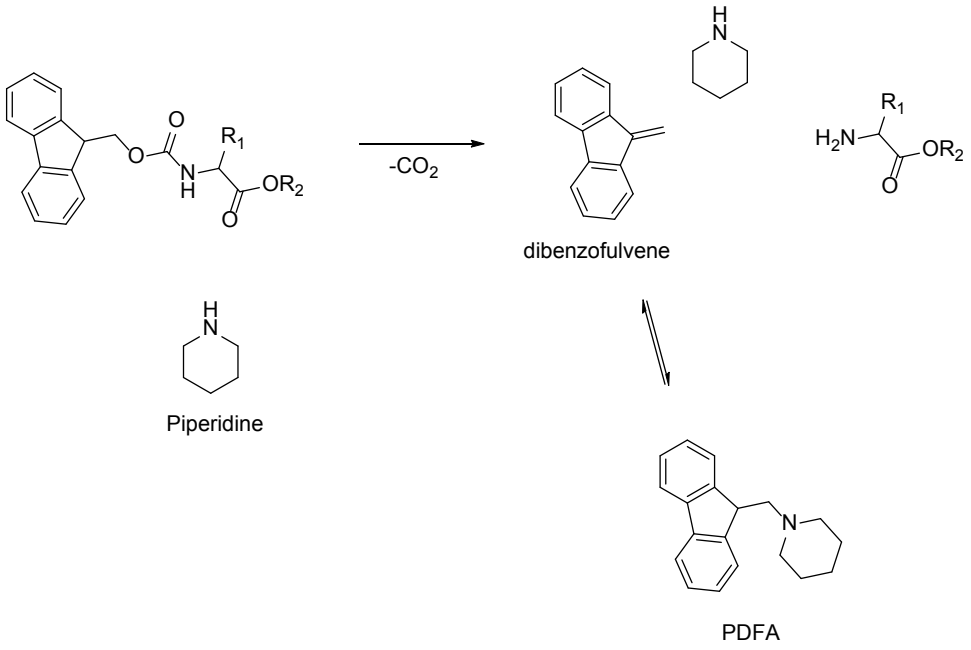

Figure 38: Schematic overview of Fmoc-cleavage and PDFA formation.

$$Peptide\ load = \frac{n}{A} = \frac{E \cdot V}{\varepsilon \cdot d \cdot A}$$

Equation 1: Peptide load calculated by Fmoc-cleavage; n= amount of substance in mole; A= surface area covered with deprotection solution; E= extinction; V= applied volume of deprotection solution; ε= extinction coefficient; d= path length of cuvette**.**

All absorption measurements were routinely performed by *PEPperPRINT© GmbH* as part of the quality management system.

V.4.2. Spectroscopic ellipsometry

In order to characterize different surface properties like film thickness, surface roughness, and optical constants etc. ellipsometry can be used because of its sensitivity to the change in the optical response of incident radiation that interacts with the investigated material. Typically the change in polarization due to reflection, absorption, scattering or transmission is measured. Spectroscopic ellipsometry allows film thickness measurements down to single atomic layers in a contact-free and non-destructive manner, also working under liquids.[82,87]

To yield maximum sensitivity, the angle of incidence and the wavelength of the incident beam are controlled. This procedure is referred to as *variable angle spectroscopic ellipsometry (VASE)*.

Ellipsometry uses a beam of linearly polarized light, where the s- and p-components are analyzed. s refers to the light vector component perpendicular to the plane of incidence and p to the one parallel. Coming from the light source, both components are in phase with each other. When interacting with a material, the s- and p-components are phase-shifted. The s-component is normally reflected, whereas the p-component is mostly refracted into the optically denser medium. This leads to an ellipse-like projection of the electrical field vector perpendicular to the plane of the propagated direction of the beam.[87] Ellipsometry uses not absolute, but the ratio of reflected and incident light intensities, shown in equation 2.

$$R_x = \frac{I_r^x}{I_0^x} = |r_x|^2$$

Equation 2: Ratio of reflected and incident light intensity R. I=intensity, r= *Fresnel* reflection coefficient (indices: r= reflected, x= s- or p-polarized, 0= incident).

The *Fresnel* coefficient is also linked to the components of the electric field vector *E* and the refractive indices *η* as shown in equation 3.

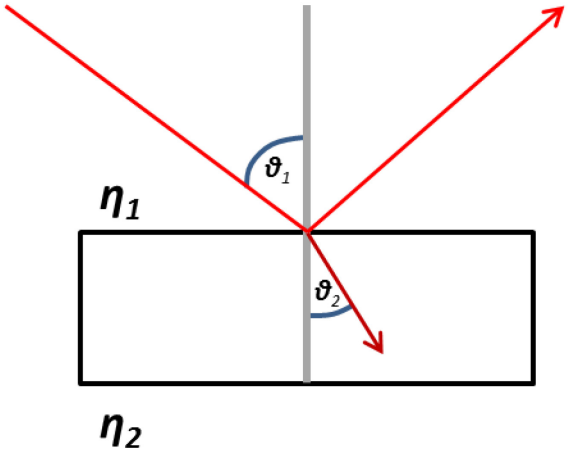

Figure 39: Reflection and refraction of a light beam at the interphase between two media.

$$r_s = \frac{E_r^s}{E_0^s} = \frac{\eta_1 \cos(\vartheta_1) - \eta_2 \cos(\vartheta_2)}{\eta_1 \cos(\vartheta_1) + \eta_2 \cos(\vartheta_2)}$$

$$r_p = \frac{E_r^p}{E_0^p} = \frac{\eta_2 \cos(\vartheta_1) - \eta_1 \cos(\vartheta_2)}{\eta_2 \cos(\vartheta_1) + \eta_1 \cos(\vartheta_2)}$$

Equation 3: *Fresnel* refraction coefficients. r= Fresnel reflection coefficient, E= component of the electric field vector, η= refractive index, ϑ= incident angle (indices: r= reflected, 0= incident, s/p= s-/p-polarized, 1= Medium A, 2= Medium B).

According to *Snell* law the ratio of the sines of the incident angles is equivalent to the opposite ratio of the refractive indices (see equation 4).

$$\frac{\sin(\vartheta_1)}{\sin(\vartheta_2)} = \frac{\eta_2}{\eta_1}$$

Equation 4: *Snell* law of refraction.

In the fundamental equation of ellipsometry, the *Fresnel* coefficients are related to the amplitude factor *ψ* and the phase factor *Δ* (see equation 5). Measuring those two factors is directly related to material properties and can be used to calculate the thickness of individual layers in multilayered systems.

$$\frac{r_p}{r_s} = \tan(\psi)e^{i\Delta}$$

Equation 5: Fundamental equation of ellipsometry. Ψ= amplitude factor, i= imaginary unit, Δ= phase factor.

In real systems however an algebraic solution is complicated because of additional parameters like surface roughness and multilayers, where the reflected light is a superposition of all beams reflected from the different interphases (see Figure 40). To solve this problem a regression analysis is required to identify those unknown parameters such as film thickness or optical constants.

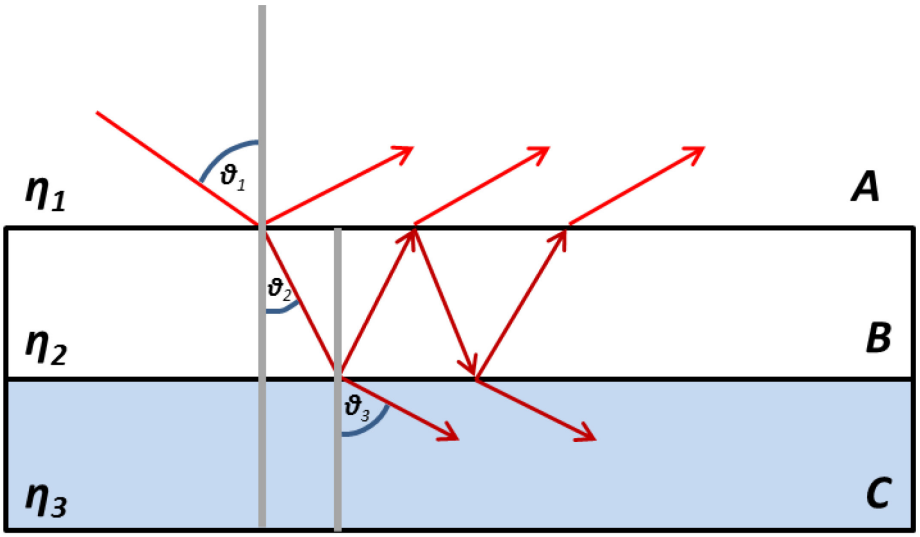

Figure 40: Reflection and refraction in a three-layer system. The incident beam is reflected and refracted at the interphase between layer A and B. The refracted beam in layer B is again reflected and refracted at the interphase between layer B and C.

In the present work ellipsometry has been used to determine the thickness of organic layers on a solid support. The *Fresnel* coefficients for such three-layer systems as depicted in Figure 35 are given in equation 6 (Layer A= Air, B= organic layer, C= solid support).

$$r_x = \frac{r_x^{12} + r_x^{23} \cdot e^{-i2\varphi}}{1 + r_x^{12} + r_x^{23} \cdot e^{-i2\varphi}}$$

$$\varphi = 2\pi \left(\frac{d}{\lambda}\right) \eta_2 \cos(\vartheta_2)$$

Equation 6: *Fresnel* reflection coefficients for a three-layer system. d= thickness of layer B with the refractive index η_2, λ= wavelength (indices: 1= layer A, 2= layer B, 3= layer C; x= s-/p-polarized).

Out of the comparison of the phase shift of a wave which is reflected at the interphase of layer A & B and B & C respectively, the thickness of layer B can be obtained. For determination of the film thickness of organic layers on a reflecting substrate, the refractive index as parameter is needed. Frequently the refractive indices of a material is unknown; in this case the *Cauchy* model can be used to parametrize the values (see equation 7).[81] To increase the accuracy, measurements are usually performed at multiple wavelengths.

$$\eta(\lambda) = \eta_0 + \frac{Y}{\lambda^2}$$

Equation 7: *Cauchy* parametrization of the refractive index. Y= *Cauchy* parameter.

For further information regarding the theoretical background as well as the technical application and setup reference is made to the literature.[82,83,87]

V.4.3. Fluorescence spectroscopy

Luminescence is the emission of light from any substance and occurs from electronically excited states. The general term can be divided into two categories, fluorescence and phosphorescence, depending on the nature of the excited state. If the electron in the excited state is of opposite spin to the one in the ground state, this state is called singlet state. The return of the excited electron back to the ground state is spin-allowed and is rapidly done by emission of a photon. Typically this process lasts around 10ns. If the electron in the excited state has the same spin orientation as the one in the ground state, this is called triplet state. The return to the ground state is in this case spin-forbidden which leads to elongated emission rates from milliseconds to seconds as phosphorescence. In general fluorescence data are presented as emission spectra, where the fluorescence intensity versus wavelength or wavenumbers is plotted. To illustrate the ongoing processes between absorption and emission, a *Jablonski* diagram is commonly used (see Figure 41).

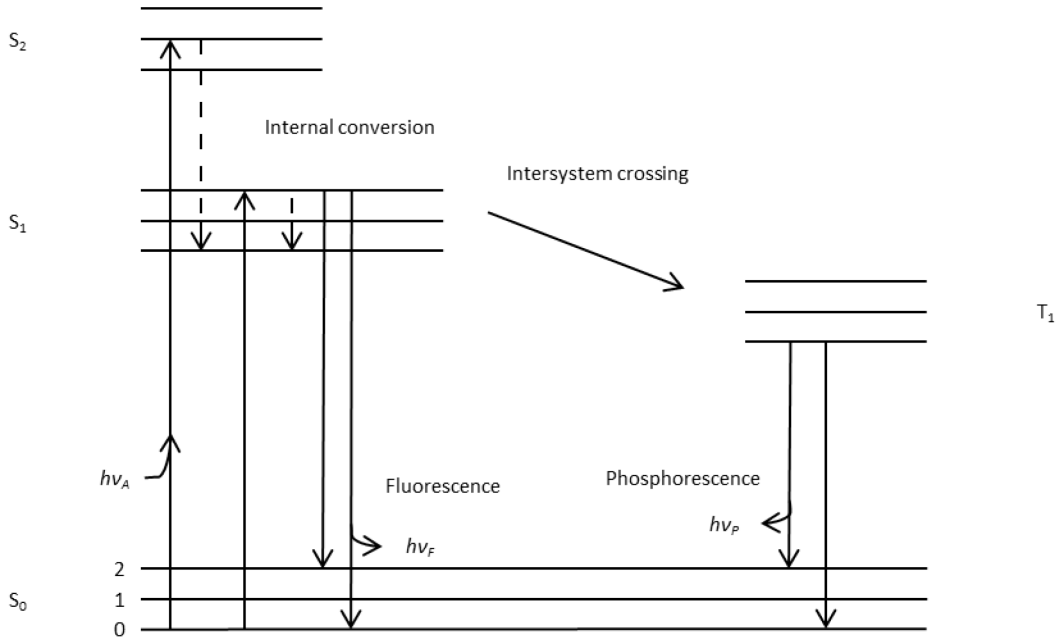

Figure 41: General form of a *Jablonski* diagram. S_0= singlet ground state, $S_{1,2}$= first/second excited singlet state, T_1= first excited triplet state, hv= energy of a photon.

At each of the electronic energy levels the fluorophore can exist in a number of vibrational levels, donated by 0, 1, 2 etc. For the influences of different parameters like quenching,

energy transfer or solvent interactions, as well as the overall theoretical background reference is made to literature.[88]

In the present work fluorescence intensity measurements of peptide microarrays were performed using common microarray scanning devices; depending on the experimental approach different organic fluorophores were used, emitting at 532/680 or 800nm.

VI. Literature

1. James, P. Protein identification in the post-genome era: the rapid rise of proteomics. *Q. Rev. Biophys.* **30,** 279–331 (1997).

2. Wilkins, M. R. *et al.* From proteins to proteomes: large scale protein identification by two-dimensional electrophoresis and amino acid analysis. *Biotechnology. (N. Y).* **14,** 61–65 (1996).

3. Neurath, H. & Walsh, K. a. Role of proteolytic enzymes in biological regulation (a review). *Proc. Natl. Acad. Sci. U. S. A.* **73,** 3825–3832 (1976).

4. López-Otín, C. & Matrisian, L. M. Emerging roles of proteases in tumour suppression. *Nat. Rev. Cancer* **7,** 800–808 (2007).

5. López-Otín, C. & Bond, J. S. Proteases: Multifunctional enzymes in life and disease. *J. Biol. Chem.* **283,** 30433–30437 (2008).

6. Degterev, A., Boyce, M. & Yuan, J. A decade of caspases. *Oncogene* **22,** 8543–8567 (2003).

7. Ehrmann, M. & Clausen, T. Proteolysis as a regulatory mechanism. *Annu. Rev. Genet.* **38,** 709–724 (2004).

8. López-Otín, C. & Overall, C. M. Protease degradomics: a new challenge for proteomics. *Nat. Rev. Mol. Cell Biol.* **3,** 509–519 (2002).

9. Hanahan, D., Weinberg, R. a & Francisco, S. The Hallmarks of Cancer Review University of California at San Francisco. **100,** 57–70 (2000).

10. Bissell, M. J. & Radisky, D. Putting tumours in context. *Nat. Rev. Cancer* **1,** 46–54 (2001).

11. Porter, D. C. *et al.* Tumor-Specific Proteolytic Processing of Cyclin E Generates Hyperactive Lower-Molecular-Weight Forms. *Mol. Cell. Biol.* **21,** 6254–6269 (2001).

12. LeBeau, A. M., Singh, P., Isaacs, J. T. & Denmeade, S. R. Prostate-specific antigen is a ‘chymotrypsin-like’ serine protease with unique P1 substrate specificity. *Biochemistry* **48,** 3490–3496 (2009).

13. Oikonomopoulou, K., Diamandis, E. P. & Hollenberg, M. D. Kallikrein-related peptidases: proteolysis and signaling in cancer, the new frontier. *Biol. Chem.* **391,** 299–310 (2010).

14. Harbeck, N. *et al.* Enhanced benefit from adjuvant chemotherapy in breast cancer patients classified high-risk according to urokinase-type plasminogen activator (uPA) and plasminogen activator inhibitor type 1 (n = 3424). *Cancer Res.* **62,** 4617–4622 (2002).

15. Taubert, H. *et al.* Co-detection of members of the urokinase plasminogen activator system in tumour tissue and serum correlates with a poor prognosis for soft-tissue sarcoma patients. *Br. J. Cancer* **102,** 731–7 (2010).

16. Iacobuzio-donahue, C. a, Shuja, S., Cai, J., Peng, P. & Jo, M. CARBOHYDRATES , LIPIDS , AND OTHER NATURAL PRODUCTS : Elevations in Cathepsin B Protein Content and Enzyme Activity Occur Independently of Glycosylation during Colorectal Tumor Progression Elevations in Cathepsin B Protein Content and Enzyme Activity Occu. *J. Biol. Chem.* **272,** 29190–29199 (1997).

17. Schweiger, A. *et al.* Serum cathepsin H as a potential prognostic marker in patients with colorectal cancer. *Int.J.Biol.Markers* **19,** 289–294 (2004).

18. Tutton, M. G. *et al.* Use of plasma MMP-2 and MMP-9 levels as a surrogate for tumour expression in colorectal cancer patients. *Int. J. Cancer* **107,** 541–550 (2003).

19. Egeblad, M. & Werb, Z. New functions for the matrix metalloproteinases in cancer progression. *Nat. Rev. Cancer* **2,** 161–174 (2002).

20. Yuan, A., Chen, J. J. -W. & Yang, P. Pathophysiology of Tumor-Associated Macrophages. **45,** 199–223 (2008).

21. Somiari, S. B. *et al.* Plasma concentration and activity of matrix metalloproteinase 2 and 9 in patients with breast disease, breast cancer and at risk of developing breast cancer. *Cancer Lett.* **233,** 98–107 (2006).

22. Ludwig, T. Local proteolytic activity in tumor cell invasion and metastasis. *Bioessays* **27,** 1181–91 (2005).

23. Jessani, N. & Cravatt, B. F. The development and application of methods for activity-based protein profiling. *Curr Opin Chem Biol* **8,** 54–59 (2004).

24. Murnane, M. J. *et al.* Active MMP-2 effectively identifies the presence of colorectal cancer. *Int. J. Cancer* **125,** 2893–902 (2009).

25. Villanueva, J. *et al.* Differential exoprotease activities confer tumor-specific serum peptidome patterns. *J. Clin. Invest.* **116,** 271–284 (2006).

26. Xia, Z. *et al.* Multiplex detection of protease activity with quantum dot nanosensors prepared by intein-mediated specific bioconjugation. *Anal. Chem.* **80,** 8649–8655 (2008).

27. Winssinger, N. *et al.* PNA-encoded protease substrate microarrays. *Chem. Biol.* **11,** 1351–1360 (2004).

28. Salisbury, C. M., Maly, D. J. & Ellman, J. a. Peptide microarrays for the determination of protease substrate specificity. *J. Am. Chem. Soc.* **124,** 14868–14870 (2002).

29. Beyer, M. *et al.* Combinatorial synthesis of peptide arrays onto a microchip. *Science* **318,** 1888 (2007).

30. Kozlov, I. a *et al.* A high-complexity, multiplexed solution-phase assay for profiling protease activity on microarrays. *Comb. Chem. High Throughput Screen.* **11,** 24–35 (2008).

31. Fodor, S. P. *et al.* Light-directed, spatially addressable parallel chemical synthesis. *Science* **251,** 767–773 (1991).

32. Heller, M. J., Forster, A. H. & Tu, E. Active microelectronic chip devices which utilize controlled electrophoretic fields for multiplex DNA hybridization and other genomic applications. *Electrophoresis* **21,** 157–164 (2000).

33. Egeland, R. D. & Southern, E. M. Electrochemically directed synthesis of oligonucleotides for DNA microarray fabrication. *Nucleic Acids Res.* **33,** 1–7 (2005).

34. Steemers, F. J., Ferguson, J. a & Walt, D. R. Screening unlabeled DNA targets with randomly ordered fiber-optic gene arrays. *Nat. Biotechnol.* **18,** 91–94 (2000).

35. Steemers, F. J. & Gunderson, K. L. Whole genome genotyping technologies on the BeadArray??? platform. *Biotechnol. J.* **2,** 41–49 (2007).

36. LaFratta, C. N. & Walt, D. R. Very high density sensing arrays. *Chem. Rev.* **108,** 614–637 (2008).

37. MacBeath, G. & Schreiber, S. L. Printing proteins as microarrays for high-throughput function determination. *Science* **289,** 1760–1763 (2000).

38. Berrade, L., Garcia, A. E. & Camarero, J. a. Protein microarrays: Novel developments and applications. *Pharm. Res.* **28,** 1480–1499 (2011).

39. Volkmer, R. Synthesis and application of peptide arrays: Quo vadis SPOT technology. *ChemBioChem* **10,** 1431–1442 (2009).

40. Breitling, F., Nesterov, A., Stadler, V., Felgenhauer, T. & Bischoff, F. R. High-density peptide arrays. *Mol. Biosyst.* **5,** 224–234 (2009).

41. Frank, R. The SPOT-synthesis technique. *J. Immunol. Methods* **267,** 13–26 (2002).

42. Hilpert, K., Winkler, D. F. H. & Hancock, R. E. W. Peptide arrays on cellulose support: SPOT synthesis, a time and cost efficient method for synthesis of large numbers of peptides in a parallel and addressable fashion. *Nat. Protoc.* **2,** 1333–49 (2007).

43. Dikmans, A. J., Beutling, U., Schmeisser, E., Thiele, S. & Frank, R. SC2: A Novel Process for Manufacturing Multipurpose High-Density Chemical Microarrays. *QSAR Comb. Sci.* **25,** 1069–1080 (2006).

44. Panganiban, L. C. *et al.* 5,449,754. **341,** (1995).

45. Agilent Technologies. Agilent SurePrint G3 Human Catalog CGH Microarrays. *Agilient Technologies Product Note* (2011). at <http://www.chem-agilent.com/pdf/5990-3368en_lo.pdf>

46. Lipshutz, R. J., Fodor, S. P., Gingeras, T. R. & Lockhart, D. J. High density synthetic oligonucleotide arrays. *Nat. Genet.* **21,** 20–4 (1999).

47. Pellois, J. P. *et al.* Individually addressable parallel peptide synthesis on microchips. *Nat. Biotechnol.* **20,** 922–926 (2002).

48. Mandal, S., Rouillard, J. M., Srivannavit, O. & Gulari, E. Cytophobic surface modification of microfluidic arrays for in situ parallel peptide synthesis and cell adhesion assays. *Biotechnol. Prog.* **23,** 972–978 (2007).

49. Stadler, V. *et al.* Combinatorial synthesis of peptide arrays with a laser printer. *Angew. Chemie - Int. Ed.* **47,** 7132–7135 (2008).

50. Chan, W. C. & White, P. D. *Fmoc Solid Phase Peptide Synthesis*. *Molecular Biology* 368 (2000). at <http://scholar.google.com/scholar?hl=en&btnG=Search&q=intitle:Fmoc+solid+phase+peptide+synthesis#1>

51. Stadler, V. PEPperPRINT GmbH. at <www.pepperprint.com>

52. Pusch, W., Flocco, M. T., Leung, S.-M., Thiele, H. & Kostrzewa, M. Mass spectrometry-based clinical proteomics. *Pharmacogenomics* **4,** 463–76 (2003).

53. Koomen, J. M. *et al.* Direct tandem mass spectrometry reveals limitations in protein profiling experiments for plasma biomarker discovery. *J. Proteome Res.* **4,** 972–81 (2005).

54. Hortin, G. L. The MALDI-TOF mass spectrometric view of the plasma proteome and peptidome. *Clin. Chem.* **52,** 1223–1237 (2006).

55. Findeisen, P. & Neumaier, M. Mass spectrometry based proteomics profiling as diagnostic tool in oncology: current status and future perspective. *Clin Chem Lab Med* **47,** 666–684 (2009).

56. Findeisen, P. *et al.* Serum amyloid A as a prognostic marker in melanoma identified by proteomic profiling. *J. Clin. Oncol.* **27,** 2199–2208 (2009).

57. Hoffman, S. a., Joo, W. a., Echan, L. a. & Speicher, D. W. Higher dimensional (Hi-D) separation strategies dramatically improve the potential for cancer biomarker detection in serum and plasma. *J. Chromatogr. B Anal. Technol. Biomed. Life Sci.* **849,** 43–52 (2007).

58. Lee, H.-J., Lee, E.-Y., Kwon, M.-S. & Paik, Y.-K. Biomarker discovery from the plasma proteome using multidimensional fractionation proteomics. *Curr. Opin. Chem. Biol.* **10,** 42–9 (2006).

59. Findeisen, P., Peccerella, T., Post, S., Wenz, F. & Neumaier, M. Spiking of serum specimens with exogenous reporter peptides for mass spectrometry based protease profiling as diagnostic tool. *Rapid Commun. Mass Spectrom.* **22,** 1223–9 (2008).

60. Villanueva, J. *et al.* A sequence-specific exopeptidase activity test (SSEAT) for 'functional' biomarker discovery. *Mol. Cell. Proteomics* **7,** 509–518 (2008).

61. Peccerella, T. *et al.* Endoprotease profiling with double-tagged peptide substrates: A new diagnostic approach in oncology. *Clin. Chem.* **56,** 272–280 (2010).

62. Gordon, S. G. & Benson, B. Analysis of serum cancer procoagulant activity and its possible use as a tumor marker. *Thromb. Res.* **56,** 431–40 (1989).

63. Schaal, R., Kupfahl, C., Buchheidt, D., Neumaier, M. & Findeisen, P. Systematic identification of substrates for profiling of secreted proteases from Aspergillus species. *J. Microbiol. Methods* **71,** 93–100 (2007).

64. Han, S. Y. & Kim, Y. A. Recent development of peptide coupling reagents in organic synthesis. *Tetrahedron* **60,** 2447–2467 (2004).

65. Gonnelli, M. & Strambini, G. B. Intramolecular quenching of tryptophan phosphorescence in short peptides and proteins. *Photochem. Photobiol.* **81,** 614–622 (2005).

66. Yepes, D. Ex-vivo evaluation of tumor-associated serum proteases using different synthetic peptide library approaches. (University of Heidelberg, 2013).

67. Collart, F. R. & Weiss, S. Bioconj. Chem. *Bioconj. Chem.* **19,** 786 (2008).

68. Köhn, M. *et al.* Staudinger Ligation: A New Immobilization Strategy for the Preparation of Small-Molecule Arrays. *Angew. Chemie - Int. Ed.* **42,** 5830–5834 (2003).

69. Tsien, R. Y. The green fluorescent protein. *Annu. Rev. Biochem.* **67,** 509–544 (1998).

70. Griffin, B. a, Adams, S. R. & Tsien, R. Y. Specific covalent labeling of recombinant protein molecules inside live cells. *Science* **281,** 269–272 (1998).

71. Münster, B. Entwicklung von Mikropartikeln für die hochdichte kombinatorische Peptidarraysynthese durch laserbasierte Verfahren. (Karlsruher Institut für Technologie, 2015).

72. Brizzard, B. Epitope tagging. *Biotechniques* **44,** 693–695 (2008).

73. Hebbes, T. R., Turner, C. H., Thorne, a. W. & Crane-Robinson, C. A 'minimal epitope' anti-protein antibody that recognises a single modified amino acid. *Mol. Immunol.* **26,** 865–873 (1989).

74. Wolf, J. The Properties Protein. **89,** 1–5 (1964).

75. Lynen, F., Knappe, J., Lorch, E., Jütting, G. & Ringelmann, E. Die biochemische Funktion des Biotins. *Angew. Chemie* **71,** 481–486 (1959).

76. Stadler, V. *et al.* PEGMA/MMA copolymer graftings: Generation, protein resistance, and a hydrophobic domain. *Langmuir* **24,** 8151–8157 (2008).

77. Piehler, J., Brecht, A., Hehl, K. & Gauglitz, G. Protein interactions in covalently attached dextran layers. *Colloids Surfaces B Biointerfaces* **13,** 325–336 (1999).

78. Luo, K., Zhou, P. & Lodish, H. F. The specificity of the transforming growth factor beta receptor kinases determined by a spatially addressable peptide library. *Proc. Natl. Acad. Sci. U. S. A.* **92,** 11761–11765 (1995).

79. Lee, M. H., Brass, D. a., Morris, R., Composto, R. J. & Ducheyne, P. The effect of non-specific interactions on cellular adhesion using model surfaces. *Biomaterials* **26,** 1721–1730 (2005).

80. Gunda, N. S. K., Singh, M., Norman, L., Kaur, K. & Mitra, S. K. Optimization and characterization of biomolecule immobilization on silicon substrates using (3-aminopropyl)triethoxysilane (APTES) and glutaraldehyde linker. *Appl. Surf. Sci.* **305,** 522–530 (2014).

81. Cauchy, A. L. Sur la Réfraction et la Réflexion de la lumiére. *Bulletin de Ferrusac* **14,** 6–10 (1830).

82. Vedam, K. Spectroscopic ellipsometry: a historical overview. *Thin Solid Films* **313-314,** 1–9 (1998).

83. Fujiwara, H. *Spectroscopic Ellipsometry: Principles and Applications*. *Spectroscopic Ellipsometry: Principles and Applications* 1–369 (2007). doi:10.1002/9780470060193

84. Beyer, M., Felgenhauer, T., Ralf Bischoff, F., Breitling, F. & Stadler, V. A novel glass slide-based peptide array support with high functionality resisting non-specific protein adsorption. *Biomaterials* **27,** 3505–3514 (2006).

85. Bouguer, P. {E}ssai d'optique, {S}ur la gradation de la lumière. *Claude Jombert* 164 ff. (1729). doi:10.1038/111320b0

86. Swinehart, D. F. The Beer-Lambert Law. *J. Chem. Educ.* **39,** 333 (1962).

87. Brundle, C. R., Charles A. Evans, J., Wihon, S. & Fitzpatrick, L. E. Encyclopedia of Materials Characterization. Surfaces, Interfaces, Thin Films. *Materials Characterization Series* (1992). doi:10.1002/9783527670772

88. Lakowicz, J. R. *Principles of fluorescence spectroscopy*. *Principles of Fluorescence Spectroscopy* 1–954 (2006). doi:10.1007/978-0-387-46312-4

VII. Appendix

VII.1. Abbreviations

% (m/v)	mass per volume fraction
% (v/v)	volume fraction
Ac_2O	acetic anhydride
APTES	(3-Aminopropyl)triethoxysilane
asp-N	endoproteinase asp-N from *Pseudomonas fragi* mutant strain
Biotin-X-NHS	6-[[5-[(3aS,4S,6aR)-hexhydro-2-oxo-1H-thieno[3,4-d]imidazol-4-yl]-1-oxopentyl]amino]-2,5-dioxo-1-pyrrolidinyl-ester-hexanoic acid
Biotin-Opfp	Biotin-pentafluorophenylester
CDI	1,1′-Carbonyldiimidazole
CM-Dextran	Carboxymethyl-dextran sodium salt
DCC	*N*,*N*′-Dicyclohexylcarbodiimide
DCM	dichloromethane
DIPEA	*N,N*-diisopropylethylamine
DMF	*N,N*-Dimethylformamide
DMSO	dimethyl sulfoxide
DTT	*threo*-1,4-Dimercapto-2,3-butanediol
e.g.	[latin] *exempli gratia*, for example
et al.	[latin] *et alii*, and others
EtOH	ethanol
ESA	acetic anhydride

FlAsH-EDT_2	Fluorescein arsenical helix binder, 4',5'-Bis(1,3,2-dithioarsolan-2-yl)fluorescein
Fmoc	9-fluorenylmethoxycarbonyl (protecting group)
GFP	green fluorescent protein
H	hour(s)
HA	Human influenza hemagglutinin
HBTU	2-(1H-benzotriazole-1-yl)-1,1,3,3-tetramethyluronium hexafluorophosphate
HOBt	1-hydroxybenzotriazol
MeCN	acetonitrile
MeOH	methanol
Min	minute(s)
MMA	methylmethacrylate
mpSPPS	micro particle-based solid phase peptide synthesis
M_W	molecular weight
NHS	1-Hydroxy-2,5-pyrrolidinedione
NIH	National Institute of Health standard, one "NIH" unit is equivalent to 1.1 to 1.3 IU (international unit) of thrombin
Opfp	orthopentafluorophenyl moiety
PBS-T	phosphate buffer saline with additional Tween20
PDFA	piperidinedibenzofulvene adduct
PEG	poly(ethylene glycol)
PEGMA	poly(ethylene glycol) methacrylate
PMT	photomultiplier tube
^{i}PrOH	2-propanol
PVP	polyvinylpyrrolidone

RT	room temperature (here 23 °C)
SMCC	succinimidyl-trans-4-(*N*-maleimidylmethyl)cyclohexane-1-carboxylate
S_N2	nucleophilic substitution
TAMRA	5(6)-carboxytetramethyl rhodamine
TBS-T	TRIS buffer saline with additional Tween20
TFA	trifluoroaceticacid
TRIS	Triisopropylsilane
Tween20	polyoxyethylensorbitan monolaurate (surfactant)
UV/Vis	ultra-violet/visible

VII.2. Amino acid codes

Ala	A	alanine
Arg	R	arginine
Asn	N	asparagine
Asp	D	aspartic acid
Cys	C	cysteine
Gln	Q	glutamine
Glu	E	glutamic acid
Gly	G	glycine
His	H	histidine
Ile	I	isoleucine
Leu	L	leucine
Lys	K	lysine
Met	M	methionine
Phe	F	phenylalanine
Pro	P	proline
Ser	S	serine
Thr	T	threonine
Trp	W	tryptophan
Tyr	Y	tyrosine
Val	V	valine

VII.3. Funding

This work was supported by:

The *Deutsche Krebshilfe* (project number 110171).

VII.4. Danksagung

Für die exzellente Betreuung der Doktorarbeit und die Begleitung im Rahmen des DKFZ *International PhD-program* als *Thesis adisory comitee* (TAC), danke ich PD Dr. F. Ralf Bischoff (DKFZ), Prof. (apl.) Dr. Reiner Dahint (*Angewandte physikalische Chemie*, Universität Heidelberg) und Dr. Martina Schnölzer (DKFZ), die mir stets mit Rat und Tat zur Seite standen.

Mein Dank gilt der *deutschen Krebshilfe*, die das Projekt erst möglich gemacht hat, sowie der finanziellen Unterstützung durch die gesamte Arbeitsgruppe *funktionelle Genomanalyse* des DKFZ.

Besonderer Dank gilt allen Kollegen der Arbeitsgruppe *funktionelle Genomanalyse* am DKFZ, der Firmenausgründung *PEPperPRINT GmbH*, den Kollegen des *Instituts für klinische Chemie* (IKC) am Universitätsklinikum Mannheim, den Kollegen der Abteilung *Peptidarrays und Antikörperbibliotheken* am Karlsruher Institut für Technologie (KIT) und den Kooperationspartnern vom *Institut für Mikrosystemtechnik* (IMTEK) an der Universität Freiburg. Namentlich: PD Dr. F. Ralf Bischoff, Dr. Jörg Hoheisel, Prof. Dr. med. Peter Findeisen, Prof. Dr. med. Michael Neumaier, Dr. Thomas Brandstetter, Dr. Volker Stadler, Dr. Thomas Felgenhauer, Dr. Diego F. Yepes, Dr. Christopher Schirwitz, Dr. Felix Löffler, Dr. Victor Costina, Bastian Münster, Christina Lehrer, Jürgen Kretschmer, Janek Kibat, Patrick Kunz, Daniela Rambow.

Für die großartige Unterstützung und Zusammenarbeit danke ich auch meiner Arbeitsgruppe am Institut für *Angewandte Physikalische Chemie* der Universität Heidelberg: Prof. (apl.) Reiner Dahint, Dr. Anna Grab, Dr. Haci Osman Güvenc, Dr. Mustafa Sayin, Felicitas Schwörer und André Brink.

Ebenso möchte ich der Abteilung von Prof. Dr. Stefan Wiemann für die Unterstützung, den wissenschaftlichen Austausch und Bereitstellung von Geräten danken.

Von ganzem Herzen danke ich meiner Familie und meinen Freunden, insbesondere Max und Annika für die großartige Unterstützung in allen Lebenslagen und den Rückhalt, den sie mir stets geben.

Nicht zuletzt möchte ich diese Arbeit meiner verstorbenen Mutter Sibylle widmen, die viel zu früh von uns gegangen ist. Möge sie in Frieden ruhen!

VII.5. Eidesstattliche Erklärung

Erklärungen gemäß §8 (3) b) und c) der Promotionsordnung

a) Hiermit erkläre ich, dass ich die vorgelegte Dissertation selbst verfasst und mich keiner anderen als der von mir ausdrücklich bezeichneten Quellen und Hilfen bedient habe.
b) Des Weiteren erkläre ich, dass ich an keiner anderen Stelle ein Prüfungsverfahren beantragt bzw. die Dissertation in dieser oder anderer Form bereits anderweitig als Prüfungsarbeit verwendet oder einer anderen Fakultät als Dissertation vorgelegt habe.

Heidelberg, den 03.12.2015

Eric Dyrcz